Contemporary Mathematics
https://ojs.wiserpub.com/index.php/CM/

Research Article

Modeling Lifetime Data with the New Marshall-Olkin Weibull-Rayleigh Distribution and Its Bivariate Form

Zakiah I. Kalantan[1], **Abeer A. EL-Helbawy**[2*]

[1] Department of Statistics, Faculty of Science, King Abdulaziz University, Jeddah, 21589, Saudi Arabia
[2] Department of Statistics, Faculty of Commerce, AL-Azhar University (Girls' Branch), Cairo, 11865, Egypt
E-mail: abeer@azhar.edu.eg

Received: 6 May 2025; **Revised:** 5 July 2025; **Accepted:** 15 July 2025

Abstract: Lifetime distributions are indispensable in various scientific applications, particularly for analyzing bivariate measurements in reliability, engineering, and biomedical sciences. This paper introduces novel univariate and bivariate Marshall-Olkin Weibull models. Specifically, the Marshall-Olkin Weibull-Rayleigh distribution is proposed, offering enhanced flexibility to accommodate diverse univariate hazard rate shapes, including increasing, decreasing, and bathtub curves. Its novel bivariate form, the bivariate Marshall-Olkin Weibull-Rayleigh distribution, is derived using the Farlie-Gumbel-Morgenstern (FGM) copula function, designed to effectively capture various dependence structures in paired lifetime data. For parameter estimation, a comprehensive investigation is conducted comparing maximum likelihood estimation and Two-stage estimation to establish robust and efficient strategies. Furthermore, an accurate methodology for assessing copula goodness-of-fit is applied, detailing the empirical process approach, the use of pseudo-observations, and the Cramer-von Mises test statistic. Theoretical results are numerically examined through simulation. Finally, the superior performance and practical utility of the proposed bivariate Marshall-Olkin Weibull-Rayleigh model are demonstrated through a thorough analysis of real-world datasets and a comparative study against other established distributions, showcasing its significant advantages in reliability engineering applications.

Keywords: Marshall Olkin Weibull G distributions, Marshall Olkin Weibull Rayleigh distribution, bivariate Marshall Olkin Weibull Rayleigh distribution, copula, maximum likelihood method, two-stage estimation

MSC: 62N05, 62H10, 62F10

1. Introduction

Researchers have extensively focused on developing novel methodologies to generate expanded families of probability distributions, by augmenting existing baseline distributions with additional parameters like shape or scale. These efforts encompass various strategies, including general methods for parameter addition [1–6], extensions based on the Marshall-Olkin framework [2, 7, 8], and constructions involving T-X or Weibull-G classes [4, 9–13]. The field has also seen the development of practical tools, such as comprehensive R packages for working with these new families [14]. Further details on these diverse generation methods can be found in a range of dedicated studies [15–20].

DOI: https://doi.org/10.37256/cm.6520257179

Regarding Bayesian inference with censored lifetime data, [21] provided a framework for estimation and prediction concerning a flexible Weibull model under a Type-II censoring scheme, while [22] developed a method for Bayesian prediction of future observations from an inverse Weibull distribution based on Type-II hybrid censored samples.

This paper introduces novel univariate and bivariate Marshall-Olkin Weibull-Rayleigh (MOWR) models. These newly developed models feature MOWR marginal distributions, offering significant flexibility both in the marginal distributions themselves and in their dependence structure. Furthermore, these distributions have potential applications across various fields.

The Weibull-G (WG) Probability Density Function (PDF) is given by:

$$f(t,\ \mu,\ \beta,\ \delta) = \frac{\mu}{\beta}\frac{g(t,\ \delta)}{1-G(t,\ \delta)}\left\{-\frac{\log[1-G(t,\ \delta)]}{\beta}\right\}^{\mu-1}\exp\left\{-\left[-\frac{\log[1-G(t,\ \delta)]}{\beta}\right]^{\mu}\right\}, \quad t \geq 0 \tag{1}$$

Here, $G(t,\ \delta)$ and $g(t,\ \delta)$ represent the Cumulative Distribution Function (CDF) and PDF, respectively, of any baseline distribution that depends on a parameter vector δ. The variable t is within the range of $g(t,\ \delta)$, $\beta > 0$ is the scale parameter, and $\mu > 0$ is the shape parameter.

The CDF for the WG distribution is then given by:

$$F(t,\ \mu,\ \beta,\ \delta) = 1-\exp\left\{-\left[-\frac{\log[1-G(t,\ \delta)]}{\beta}\right]^{\mu}\right\}, \quad t \geq 0. \tag{2}$$

As detailed by [14, 15], the core functions of the WG distribution, including its PDF, CDF, quantile function, and methods for random number generation, are well-established. The literature features diverse classes of WG distributions, such as the Weibull-Pareto proposed by [5], and studies investigating computational aspects like negative log-likelihood minimization and convergence status for various WG distributions [6]. Additionally, [15] provides a comprehensive analysis, describing the PDF, CDF, quantile function, and key inference measures including maximum likelihood estimates, and the Bayesian Information Criterion (BIC), Cramér-von Misses, and Akaike Information Criterion (AIC), for each of these nineteen families.

Studies on various classes of WG distributions are prominent in the literature. For instance, [5] introduced the Weibull-Pareto distribution, while [11] proposed the Weibull exponentiated exponential distribution. Beyond specific distributions, [6] has investigated crucial methodological aspects, such as the minimum value of the negative log-likelihood function and the convergence status for WG distributions. Moreover, [14] conducted a comprehensive characterization of nineteen distinct families of G distributions, detailing their probability density functions, cumulative distribution functions, quantile functions, and associated inference measures (including maximum likelihood estimates, BIC, Cramér-von Misses, and AIC).

The PDF for the Marshall-Olkin Weibull-G (MOWG) distribution is given by:

$$f(t,\ \alpha,\ \mu,\ \beta,\ \delta) = \frac{\frac{\alpha\mu}{\beta}\frac{g(t,\ \delta)}{1-G(t,\ \delta)}\left\{-\frac{\log[1-G(t,\ \delta)]}{\beta}\right\}^{\mu-1}\exp\left\{-\left[-\frac{\log[1-G(t,\ \delta)]}{\beta}\right]^{\mu}\right\}}{\left\{1-\bar{\alpha}\exp\left\{-\left[-\frac{\log[1-G(t,\ \delta)]}{\beta}\right]^{\mu}\right\}\right\}^{2}}, \quad t \geq 0, \tag{3}$$

where $G(t,\ \delta)$ and $g(t,\ \delta)$ represent the CDF and PDF, respectively, of any baseline distribution that depends on a parameter vector δ. The variable t is within the range of $g(t,\ \delta)$, $\beta > 0$ is the scale parameter, and $\mu > 0$ is the shape parameter.

The CDF for the MOWG distribution is then given by:

$$F(t,\ \alpha,\ \mu,\ \beta,\ \delta) = \frac{1-\exp\left\{-\left[-\dfrac{\log[1-G(t,\ \delta)]}{\beta}\right]^{\mu}\right\}}{1-\bar{\alpha}\exp\left\{-\left[-\dfrac{\log[1-G(t,\ \delta)]}{\beta}\right]^{\mu}\right\}}, \quad t \geq 0. \tag{4}$$

Therefore, the quantile function for the MOWG distribution is expressed as:

$$F^{-1}(P,\ \delta) = G^{-1}\left(1-\exp\left\{-\beta\left[-\log\left(1-\frac{\alpha p}{\bar{\alpha}p}\right)\right]^{1/C}\right\}\right), \quad t \geq 0,\ 0 \leq p \leq 1. \tag{5}$$

The Hazard Rate Function (HRF) for the MOWG distribution is

$$h(t,\ \alpha,\ \beta,\ \mu,\ \delta) = \frac{\dfrac{\mu\alpha}{\beta}\dfrac{g(t,\ \delta)}{1-G(t,\ \delta)}\left\{-\dfrac{\log[1-G(t,\ \delta)]}{\beta}\right\}^{\mu-1}\exp\left\{-\left[-\dfrac{\log[1-G(t,\ \delta)]}{\beta}\right]^{\mu}\right\}}{1-\dfrac{1-\exp\left\{-\left[-\dfrac{\log[1-G(t,\ \delta)]}{\beta}\right]^{\mu}\right\}}{1-\bar{\alpha}\exp\left\{-\left[-\dfrac{\log[1-G(t,\ \delta)]}{\beta}\right]^{\mu}\right\}}}. \tag{6}$$

Consistent with the methodology outlined by [15], methods for generating random numbers for the MOWG distribution can be directly derived from its PDF, CDF, and quantile function. This approach aligns with the broader utility of copulas, which offer a versatile framework for constructing multivariate distributions and analyzing dependence among random variables, proving invaluable in addressing various significant problems. Consequently, a substantial body of research exists on bivariate and multivariate lifetime distributions developed using diverse construction techniques and copula functions (for more details, see [23, 24]). Recent developments in bivariate distributions are extensively covered in the literature, for example, by [25–37].

Extending the framework of bivariate Weibull-G distributions, notably the investigations by [29] into models with varying shape parameters (e.g., Weibull-Uniform, Weibull-Exponential, Weibull-Chi-square, and Weibull-Rayleigh), this paper proposes the bivariate Marshall-Olkin Weibull-Rayleigh (BMOWR) models. These models are developed using the Farlie-Gumbel-Morgenstern (FGM) copula, and the research focuses on determining the most appropriate among them. The efficacy of the proposed BMOWR model is then rigorously assessed through extensive simulation studies and real-world data analyses.

This paper aims to address existing gaps in the literature by presenting several key contributions to the field of lifetime data modeling and analysis:

• The MOWR model offers increased flexibility for analyzing univariate and bivariate lifetime data, accommodating various hazard rate shapes including increasing, decreasing, and bathtub curves.

• BMOWR model using the FGM copula is specifically designed to capture diverse dependence structures in paired lifetime data, addressing limitations in existing bivariate models.

• The performance of the Maximum Likelihood Estimation (MLE) and Two-Stage Estimation (TSE) methods is compared to provide robust and efficient estimation strategies for the proposed model.

• An application of the empirical process approach for assessing copula goodness-of-fit. This includes the accurate use of pseudo-observations and the Cramer-von Mises test statistic, offering a robust framework for validating the bivariate model.

• The applicability and superior performance of the proposed BMOWR model are achieved through a thorough analysis of a real-world dataset and a comparative study against other established bivariate models, thereby showcasing its utility and advantages in reliability engineering.

Accurately modeling lifetime data is fundamental across diverse scientific and engineering disciplines, particularly in reliability analysis, biomedical research, and complex system design. Many real-world systems, however, involve components with inherently interdependent lifetimes, where assuming independence often leads to inaccurate predictions and suboptimal decision-making. Existing bivariate lifetime models frequently lack the necessary flexibility to simultaneously capture the complex and varied hazard rate behaviors of individual components and the intricate dependence structures between them. Addressing this critical gap, this paper introduces a novel and highly versatile BMOWR distribution. Constructed using the FGM copula, the BMOWR model offers unprecedented flexibility in modeling bivariate HRF shapes, including the crucial increasing, decreasing, and bathtub curves, which are vital for understanding joint degradation processes. Furthermore, it effectively captures diverse dependence structures between component lifetimes. We carefully explore its structural properties and propose robust parameter estimation strategies using both MLE and TSE methods. Extensive simulation studies validate the estimators' performance, and real-world data analyses quantitatively demonstrate the BMOWR's superior fit and applicability compared to established benchmarks. This work thus provides a powerful new tool for reliability engineering, biomedical research, and other fields requiring accurate modeling of interdependent lifetime data.

This article is structured as follows: Section 2 details the proposed new MOWR model. Section 3 introduces a novel BMOWR model derived using the FGM copula function. The estimation of the BMOWR model's parameters using the MLE and TSE methods is covered in section 4. Section 5 introduces the methodology for assessing the goodness-of-fit of copula models, detailing the empirical process approach, the use of pseudo-observations, and the Cramér-von Mises test statistic for comparing parametric and empirical copulas. A real-world dataset is analyzed in section 6 to illustrate the performance of the suggested bivariate model and compare it with other bivariate models. Section 8 gives concluding remarks. Suggestions for future research are provided in section 9.

2. Univariate Marshall Olkin Weibull Rayleigh distribution

This section presents and studies the MOWR distribution. Considering that t has the Rayleigh distribution, then

$$g(t;\,\lambda) = 2\frac{t}{\lambda^2}\exp\left(-\frac{t^2}{\lambda^2}\right), \quad 0 < t < \lambda < \infty \tag{7}$$

and

$$G(t;\,\lambda) = 1 - \exp\left(-\frac{t^2}{\lambda^2}\right) \tag{8}$$

Consequently, the PDF and CDF of the MOWR distribution are given by, respectively:

$$f(t,\,\alpha,\,\mu,\,\beta,\,\lambda) = \frac{\dfrac{2\alpha\mu}{\lambda^{2\mu}\beta^{\mu}}t^{2\mu-1}\exp\left\{-\left[\dfrac{t^2}{\lambda^2\beta}\right]^{\mu}\right\}}{\left\{1-\bar{\alpha}\exp\left\{-\left[\dfrac{t^2}{\lambda^2\beta}\right]^{\mu}\right\}\right\}^{2}}, \quad t,\,\alpha,\,\mu,\,\beta,\,\lambda > 0 \tag{9}$$

and

$$F(t,\ \alpha,\ \mu,\ \beta,\ \lambda) = \frac{1-\exp\left\{-\left[\frac{t^2}{\lambda^2\beta}\right]^{\mu}\right\}}{1-\bar{\alpha}\exp\left\{-\left[\frac{t^2}{\lambda^2\beta}\right]^{\mu}\right\}}, \quad t,\ \alpha,\ \mu,\ \beta,\ \lambda > 0 \tag{10}$$

The HRF for the MOWR distribution is as follows:

$$h(t,\ \alpha,\ \beta,\ \mu,\ \delta) = \frac{\frac{2\alpha\mu}{\lambda^{2\mu}\beta^{\mu}}t^{2\mu-1}\exp\left\{-\left[\frac{t^2}{\lambda^2\beta}\right]^{\mu}\right\}}{\left\{\exp\left\{-\left[\frac{t^2}{\lambda^2\beta}\right]^{\mu}\right\}-\bar{\alpha}\exp\left\{-\left[\frac{t^2}{\lambda^2\beta}\right]^{\mu}\right\}\right\}\left\{1-\bar{\alpha}\exp\left\{-\left[\frac{t^2}{\lambda^2\beta}\right]^{\mu}\right\}\right\}} \tag{11}$$

Both the MOWR and BMOWR distributions are defined over positive real numbers and involve either one or two parameters. In practical applications, utilizing these distributions provides researchers with flexibility to model datasets exhibiting diverse structures, characterized by varying shape and location parameters.

3. Bivariate Marshall Olkin Weibull Rayleigh distributions based on FGM copula

Any multivariate distribution can be separated into a copula and its continuous marginal distributions. In the bivariate setting, copulas serve to connect two marginal distributions to form their joint distribution. Further details are available in [27].

For any bivariate distribution function $F(t_1,\ t_2)$ with continuous marginals $F(t_1),\ F(t_2)$, there is a unique copula function C such that:

$$F(t_1,\ t_2) = C(F_1(t_1),\ F_2(t_2)), \quad -(t_1,\ t_2) \in (-\infty,\ \infty)\times(-\infty,\ \infty) = C(u,\ v) \tag{12}$$

where $u = F_1(t_1)$ and $v = F_2(t_2)$.

The bivariate distribution has a density function defined as:

$$f(t_1,\ t_2) = f_1(t_1)f_2(t_2)c(F_1(t_1),\ F_2(t_2)), \tag{13}$$

where $c(F_1(t_1),\ F_2(t_2))$ is the density function of the copula [38].

Various copula functions can be employed to construct BMOWG distributions with MOWG marginals as defined in (9). In this paper, we will utilize several copulas to achieve this construction. The statistical literature contains a substantial number of copulas; this article uses the FGM and Plackett copulas to derive a bivariate generalized exponential distribution. The FGM family is a widely recognized parametric family of copulas, as discussed in [38]. The distribution function for the FGM copula is given by

$$C(u,\ v) = uv[1+\theta(1-u)(1-v)] \tag{14}$$

The corresponding density function for this copula is given by

$$c(u,\ v) = [1 + \theta(2u-1)(2v-1)] \tag{15}$$

where u and v are within the unit interval I, and θ is a dependence parameter in the range of $[-1,\ 1]$. Notably, when the dependence parameter θ is zero, the FGM copula simplifies to represent independence between the variables. While the FGM copula family is mathematically convenient to work with, it has limitations in modeling strong dependencies. Specifically, Kendall's tau τ for this copula is in the range of $[-0.222,\ 0.222]$, and Spearman's rho; ρ, is in the range of $[-0.333,\ 0.333]$. The BMOWR distribution is constructed using the FGM copula. The BMOWR model, relying on the FGM copula, has a known property regarding tail dependence: the FGM copula exhibits zero (or weak) tail dependence. This means it does not effectively model situations where components tend to fail together in extreme conditions (e.g., both failing very early or both lasting exceptionally long).

Unimodal marginals are considered based on the MOWR distribution to define the BMOWR's PDF as follows:

$$\begin{aligned} f(t_1,\ t_2,\ \underline{\alpha},\ \underline{\beta},\ \underline{\lambda},\ \underline{\mu}) = \prod_{j=1}^{2} & \frac{\dfrac{2\alpha_j\mu_j}{\lambda_j^{2\mu_j}\beta_j^{\mu_j}} t_j^{2\mu_j-1} \exp\left\{-\left[\dfrac{t_j^2}{\lambda_j^2\beta_j}\right]^{\mu_j}\right\}}{\left\{1-\bar{\alpha}_j \exp\left\{-\left[\dfrac{t_j^2}{\lambda_j^2\beta_j}\right]^{\mu_j}\right\}\right\}^2} \\ & \times [1+\theta(2u-1)(2v-1)], \quad t_j,\ \alpha_j,\ \beta_j,\ \mu_j,\ \lambda_j > 0 \end{aligned} \tag{16}$$

where $\theta \in [-1,\ 1]$ is a parameter that governs the dependence between the variables.

The conditional PDF and conditional CDF of $T_1 \mid T_2$ are provided below

$$\begin{aligned} f(t_1 \mid t_2) = {} & (\alpha+1)\alpha_1(1+t_1)^{-(\alpha_1+1)}\left[1-(1+t_1)^{-\alpha_1}\right]^{-(\alpha+1)}\left[1-(1+t_2)^{-\alpha_2}\right]^{-(\alpha+1)} \\ & \times \left\{\left[1-(1+t_1)^{-\alpha_1}\right]^{-\alpha} + \left[1-(1+t_2)^{-\alpha_2}\right]^{-\alpha} - 1\right\}^{-\left(\frac{1+2\alpha}{\alpha}\right)} \end{aligned} \tag{17}$$

and

$$F(t_1 \mid t_2) = \int_0^{t_1} f(t_1 \mid t_2)dt_1 \tag{18}$$

where $f(t_1 \mid t_2)$ is given by Equation (17).

Moments are fundamental in understanding the BMOWR distribution's behavior, especially given its complex structure. The mean and variance provide a basic understanding of the distribution's central location and spread, which are crucial in applications where the BMOWR model is used, like in modeling correlated lifetime data. Skewness and kurtosis help us understand the distribution's shape and the probability of extreme events, which are vital for interpreting the dependence structure between components in a system modeled by the BMOWR.

The BMOWR distribution, due to its composition of the Weibull and Rayleigh components, typically exhibits asymmetry. This asymmetry significantly affects its mathematical properties, especially when considering its moments and the shape of its hazard rate function.

Due to the distribution's inherent composition of the Weibull and Rayleigh components, it typically exhibits significant skewness. This skewness directly affects several of its properties. It influences the distribution's moments, particularly the third moment, which quantifies skewness itself. It also impacts the shape of the hazard rate function, potentially leading to non-symmetric hazard patterns. Furthermore, the skewness can affect the performance of certain statistical inference procedures, especially when using methods that assume symmetry.

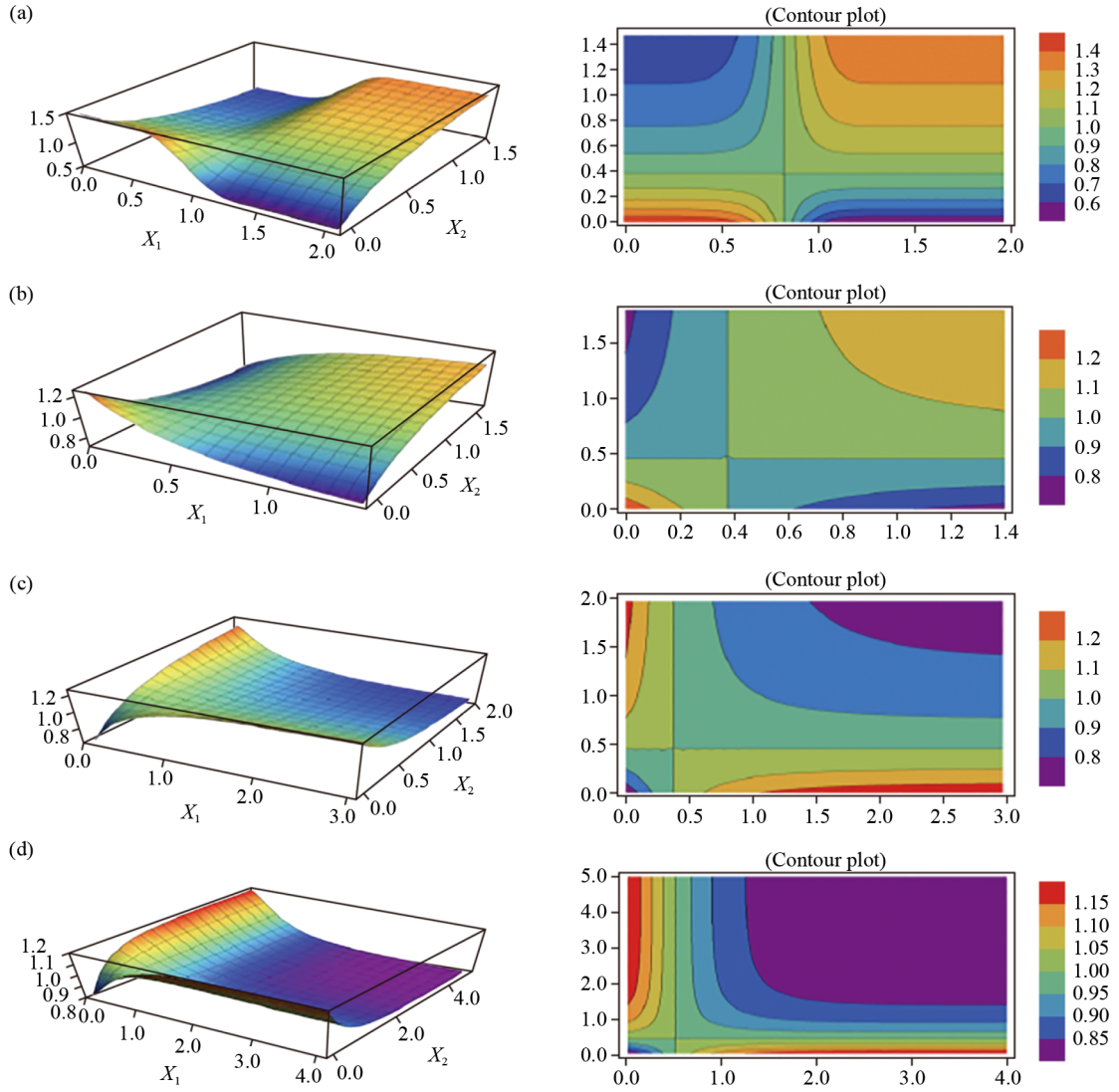

Figure 1. The plots and contour plots of the joint PDF of the BMOWR distribution for various parameter values: (a) ($\theta = 0.5$, $\alpha_1 = 0.7$, $\alpha_2 = 0.4$, $\beta_1 = 3.5$, $\beta_2 = 0.6$, $\mu_1 = 3$, $\mu_2 = 0.5$, $\lambda_1 = 0.7$, $\lambda_2 = 1.5$); (b) ($\theta = 0.3$, $\alpha_1 = 0.7$, $\alpha_2 = 0.5$, $\beta_1 = 2$, $\beta_2 = 0.2$, $\mu_1 = 0.5$, $\mu_2 = 0.5$, $\lambda_1 = 0.5$, $\lambda_2 = 2.5$); (c) ($\theta = -0.3$, $\alpha_1 = 0.7$, $\alpha_2 = 0.5$, $\beta_1 = 2$, $\beta_2 = 0.2$, $\mu_1 = 0.5$, $\mu_2 = 0.5$, $\lambda_1 = 0.5$, $\lambda_2 = 2.5$); and (d) ($\theta = 0.2$, $\alpha_1 = 0.6$, $\alpha_2 = 0.4$, $\beta_1 = 2.1$, $\beta_2 = 0.2$, $\mu_1 = 0.7$, $\mu_2 = 0.6$, $\lambda_1 = 0.6$, $\lambda_2 = 2.4$)

The kurtosis of the BMOWR distribution, which measures the 'tailedness' or peakedness, significantly influences its mathematical properties. Specifically, high kurtosis indicates heavier tails and a sharper peak, affecting the distribution's behavior in extreme value scenarios and the stability of parameter estimates.

Plots and contour plots displaying the joint PDF, CDF, Reliability Function (RF) and HRF of the BMOWR distribution are exhibited for various parameter settings in Figures 1-4, respectively.

Figure 1 shows the joint PDF of the BMOWR distribution effectively demonstrates the remarkable flexibility of the BMOWR distribution's in adapting to diverse parameter configurations. The plots illustrate a wide range of shapes, including bell-shaped (Figure 1a), inverted bell shape (Figure 1b), U-shaped characteristics or bimodal tendencies (Figure 1c) resembling complex interactions, and monotonically increasing surfaces (Figure 1d). Figure 4 displays the joint HRF of the BMOWR model which exhibits various complex shapes, including increasing, decreasing, and bathtub patterns, which provides a richer framework for modeling joint failure phenomena beyond what simpler Marshall-Olkin extensions might offer.

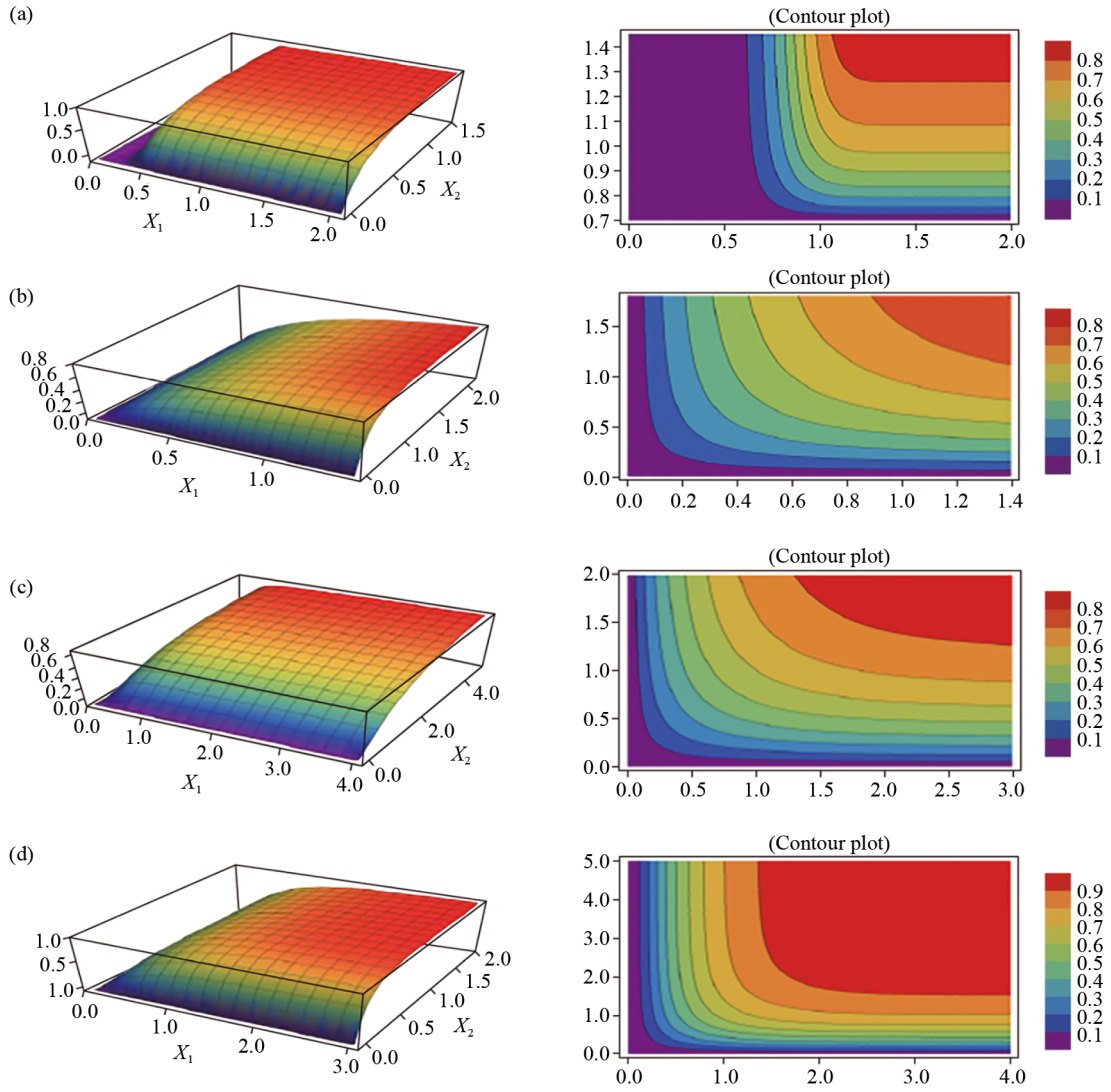

Figure 2. The plots and contour plots of the joint CDF of the BMOWR distribution for different parameter values: (a) ($\theta = 0.5$, $\alpha_1 = 0.7$, $\alpha_2 = 0.4$, $\beta_1 = 3.5$, $\beta_2 = 0.6$, $\mu_1 = 3$, $\mu_2 = 0.5$, $\lambda_1 = 0.7$, $\lambda_2 = 1.5$); (b) ($\theta = 0.3$, $\alpha_1 = 0.7$, $\alpha_2 = 0.5$, $\beta_1 = 2$, $\beta_2 = 0.2$, $\mu_1 = 0.5$, $\mu_2 = 0.5$, $\lambda_1 = 0.5$, $\lambda_2 = 2.5$); (c) ($\theta = -0.3$, $\alpha_1 = 0.7$, $\alpha_2 = 0.5$, $\beta_1 = 2$, $\beta_2 = 0.2$, $\mu_1 = 0.5$, $\mu_2 = 0.5$, $\lambda_1 = 0.5$, $\lambda_2 = 2.5$); and (d) ($\theta = -0.2$, $\alpha_1 = 0.6$, $\alpha_2 = 0.4$, $\beta_1 = 2.1$, $\beta_2 = 0.2$, $\mu_1 = 0.7$, $\mu_2 = 0.6$, $\lambda_1 = 0.6$, $\lambda_2 = 2.4$)

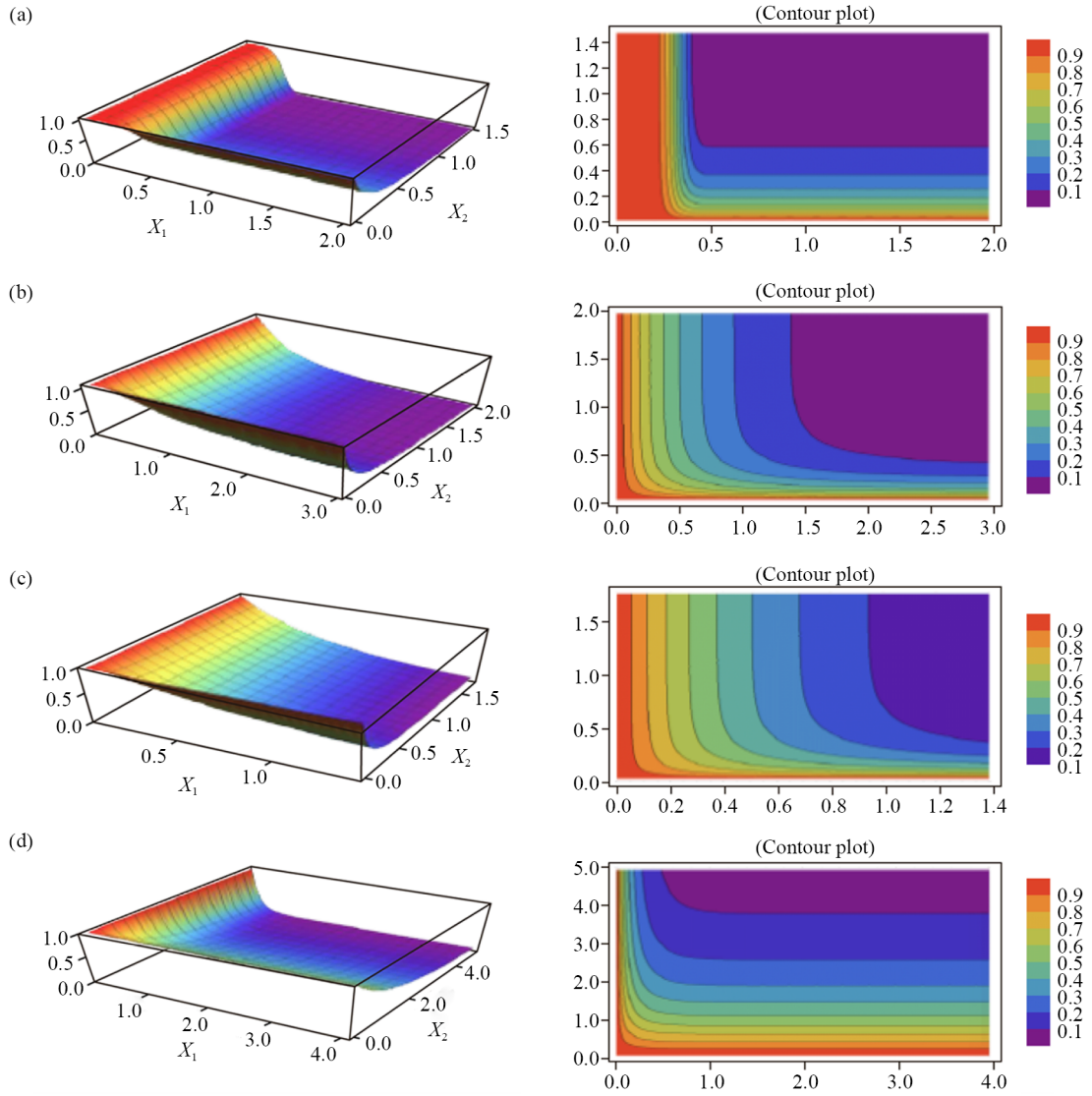

Figure 3. The plots and contour plots of the joint RF of the BMOWR distribution for different parameter values: (a) ($\theta = 0.5$, $\alpha_1 = 0.7$, $\alpha_2 = 0.4$, $\beta_1 = 3.5$, $\beta_2 = 0.6$, $\mu_1 = 3$, $\mu_2 = 0.5$, $\lambda_1 = 0.7$, $\lambda_2 = 1.5$); (b) ($\theta = 0.3$, $\alpha_1 = 0.7$, $\alpha_2 = 0.5$, $\beta_1 = 2$, $\beta_2 = 0.2$, $\mu_1 = 0.5$, $\mu_2 = 0.5$, $\lambda_1 = 0.5$, $\lambda_2 = 2.5$); (c) ($\theta = -0.3$, $\alpha_1 = 0.7$, $\alpha_2 = 0.5$, $\beta_1 = 2$, $\beta_2 = 0.2$, $\mu_1 = 0.5$, $\mu_2 = 0.5$, $\lambda_1 = 0.5$, $\lambda_2 = 2.5$); and (d) ($\theta = -0.2$, $\alpha_1 = 0.6$, $\alpha_2 = 0.4$, $\beta_1 = 2.1$, $\beta_2 = 0.2$, $\mu_1 = 0.7$, $\mu_2 = 0.6$, $\lambda_1 = 0.6$, $\lambda_2 = 2.4$)

By leveraging the FGM copula function within the BMOWR construction, explicitly decouples the marginal behavior from the dependence structure. This allows the BMOWR model to capture a wider and more flexible range of dependence patterns between the two variables than many standard Marshall-Olkin extensions, providing a more versatile tool for bivariate analysis. While the FGM copula itself has known limitations in capturing very strong dependence, its integration provides a more direct and flexible way to model mild to moderate dependence compared to some minimum-based Marshall-Olkin constructions.

The use of a flexible baseline distribution; Weibull-Rayleigh components within the Marshall-Olkin framework, combined with a copula allows for greater customization of both marginal properties and the interdependence structure independently. By addressing these specific limitations, the BMOWR model offers a more robust, flexible, and comprehensive tool for modeling complex bivariate lifetime data, significantly enhancing the capabilities available to researchers and practitioners in fields like reliability engineering.

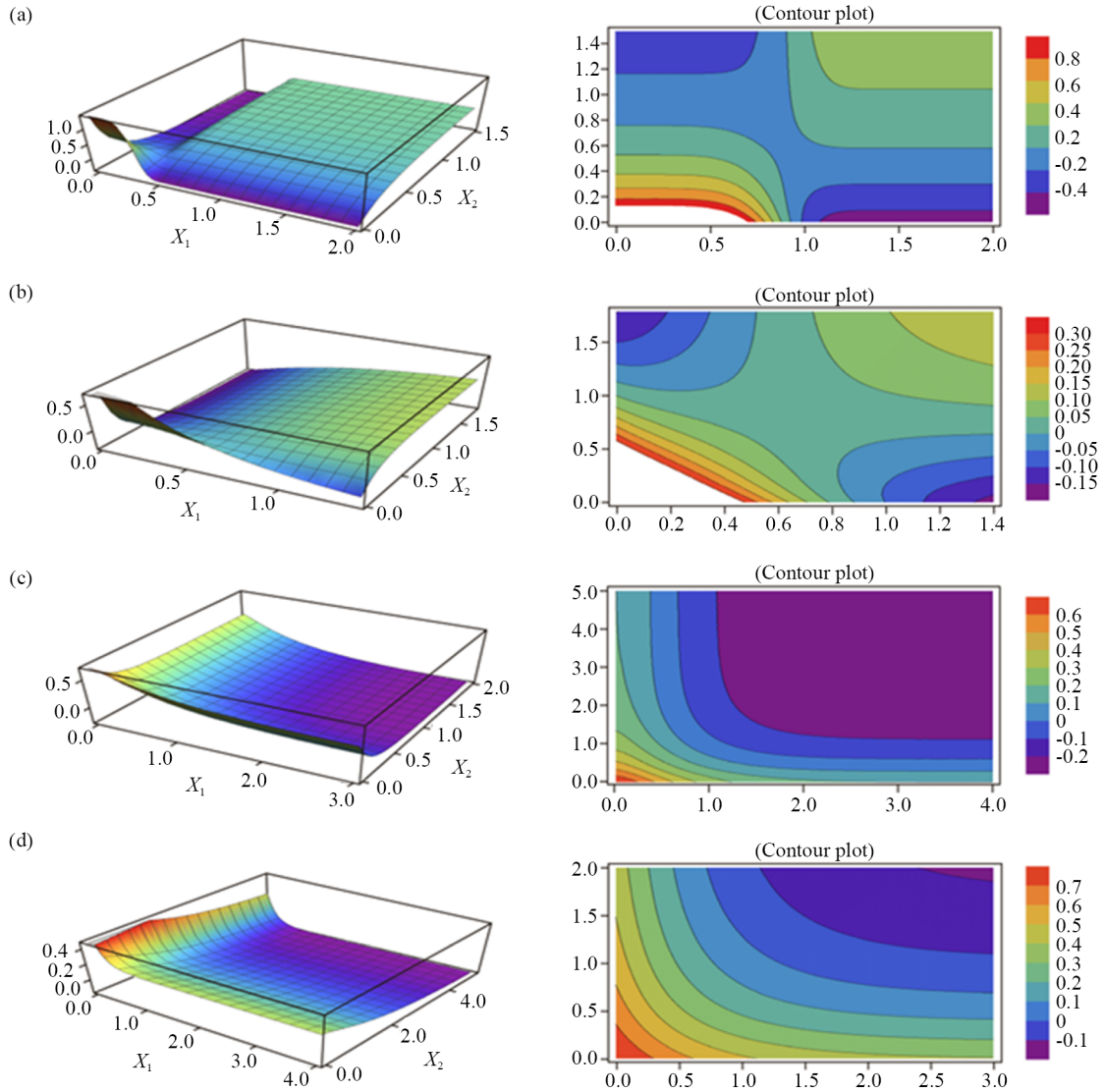

Figure 4. The plots and contour plots of the joint HRF of the BMOWR distribution for different parameter values: (a) ($\theta = 0.5$, $\alpha_1 = 0.7$, $\alpha_2 = 0.4$, $\beta_1 = 3.5$, $\beta_2 = 0.6$, $\mu_1 = 3$, $\mu_2 = 0.5$, $\lambda_1 = 0.7$, $\lambda_2 = 1.5$); (b) ($\theta = 0.3$, $\alpha_1 = 0.7$, $\alpha_2 = 0.5$, $\beta_1 = 2$, $\beta_2 = 0.2$, $\mu_1 = 0.5$, $\mu_2 = 0.5$, $\lambda_1 = 0.5$, $\lambda_2 = 2.5$); (c) ($\theta = -0.3$, $\alpha_1 = 0.7$, $\alpha_2 = 0.5$, $\beta_1 = 2$, $\beta_2 = 0.2$, $\mu_1 = 0.5$, $\mu_2 = 0.5$, $\lambda_1 = 0.5$, $\lambda_2 = 2.5$); and (d) ($\theta = -0.2$, $\alpha_1 = 0.6$, $\alpha_2 = 0.4$, $\beta_1 = 2.1$, $\beta_2 = 0.2$, $\mu_1 = 0.7$, $\mu_2 = 0.6$, $\lambda_1 = 0.6$, $\lambda_2 = 2.4$)

4. Estimation of the models' parameters and prediction

This section focuses on deriving the estimators for the parameter vector $(\alpha_j,\ \beta_j,\ \lambda_j,\ \mu_j,\ \theta)$, RF and HRF of the BMOWR models. Additionally, it presents the two-sample prediction for new observations from a future random sample drawn from the same models. The estimation of the parameters, rf, and HRF for the BMOWR model is achieved using two methods, namely, MLE and TSE, which are employed to estimate the parameters of the proposed distribution. Further details are provided in the subsequent sections.

4.1 *Parameter estimation methods*

Two distinct approaches are employed to fit copula models. The first involves a two-step procedure where the marginal distributions and the copula parameter are estimated separately. The second approach utilizes pseudo-

observations to simultaneously estimate both the marginal distributions and the copula parameter when fitting the copula model.

4.1.1 *Maximum likelihood estimation method*

This subsection outlines the parameter estimation for the BMOWR distribution using MLE by maximizing its likelihood function. This estimation is performed using a two-step procedure, where the marginal distributions and the copula parameter are estimated sequentially (separately). The resulting log-likelihood function can then be expressed as:

$$\log L = \sum_{i=1}^{n} \left[\log f_1(x_{1i}) + \log f_2(x_{2i}) + \log c(F_1(x_{1i}),\ F_2(x_{2i}))\right]. \tag{19}$$

The log-likelihood function in Equation (19) can be rewritten as follows:

$$\log L = \sum_{i=1}^{n} \log f_1(x_{1i}) + \sum_{i=1}^{n} \log f_2(x_{2i}) + \sum_{i=1}^{n} \log c(F_1(x_{1i}),\ F_2(x_{2i}))] \tag{20}$$

The initial step involves estimating the parameters of the marginal distributions F_1 and F_2 independently using MLE, as shown below:

$$\log L_j = \sum_{i=1}^{n} \log f_j(x_{ji}),\ j = 1,\ 2 \tag{21}$$

Subsequently, the copula parameters are estimated by maximizing the copula density, as follows:

$$\log L = \sum_{i=1}^{n} \log c(F_1(x_{1i}),\ F_2(x_{2i})) \tag{22}$$

Considering the first step with the BMOWR distribution, the parameters for each marginal distribution are estimated using the MLE method. If $t_1,\ \ldots,\ t_n$ represents a random sample from a MOWR distribution with parameters $(\alpha_j,\ \beta_j,\ \lambda_j,\ \mu_j)$, then the log-likelihood function $L(\alpha_j,\ \beta_j,\ \lambda_j,\ \mu_j)$ is as follows:

$$\begin{aligned}\log L_j(t_j,\ \alpha_j,\ \beta_j,\ \lambda_j,\ \mu_j) &= 2n\log(\alpha_j) - 2n\mu_j \log(\lambda_j) - n\mu_j \log(\beta_j) + n\log(\mu_j) \\ &\quad - \mu_j \sum_{i=1}^{n} \left[\frac{t_{ji}^2}{\lambda_j^2 \beta_j}\right] - 2\sum_{i=1}^{n} \log\left\{1 - \overline{\alpha_j} \exp\left\{-\left[\frac{t_{ji}^2}{\lambda_j^2 \beta_j}\right]^{\mu_j}\right\}\right\}\end{aligned} \tag{23}$$

$$\frac{\partial \log L_j(t_j,\ \alpha_j,\ \beta_j,\ \lambda_j,\ \mu_j)}{\partial \alpha_j} = \frac{2n}{\alpha_j} - \frac{2\sum_{i=1}^{n} \log\left\{1 - \overline{\alpha_j} \exp\left\{-\left[\frac{t_{ji}^2}{\lambda_j^2 \beta_j}\right]^{\mu_j}\right\}\right\} / \partial \alpha_j}{\left\{1 - \overline{\alpha_j} \exp\left\{-\left[\frac{t_{ji}^2}{\lambda_j^2 \beta_j}\right]^{\mu_j}\right\}\right\}} = 0 \tag{24}$$

$$\frac{\partial \log L_j(t_{ji},\ \alpha_j,\ \beta_j,\ \lambda_j,\mu_j)}{\partial \beta_j} = \frac{-n\mu_j}{\beta_j} + \frac{\mu_j}{\lambda_j^2\beta_j^2}\sum_{i=1}^{n} t_{ji}^2$$

$$- \frac{2\sum_{i=1}^{n}\log\left\{1-\overline{\alpha_J}\exp\left\{-\left[\frac{t_{ji}^2}{\lambda_j^2\beta_j}\right]^{\mu_j}\right\}\right\} \Big/ \partial\beta_j}{\left\{1-\overline{\alpha_J}\exp\left\{-\left[\frac{t_{ji}^2}{\lambda_j^2\beta_j}\right]^{\mu_j}\right\}\right\}} = 0 \tag{25}$$

$$\frac{\partial \log L_j(t_j,\ \alpha_j,\ \beta_j,\ \lambda_j,\ \mu_j)}{\partial \lambda_j} = \frac{-2n\mu_j}{\lambda_j} + \frac{\mu_j}{\lambda_j^3\beta_j}\sum_{i=1}^{n} t_{ji}^2$$

$$- \frac{2\sum_{i=1}^{n}\log\left\{1-\overline{\alpha_J}\exp\left\{-\left[\frac{t_{ji}^2}{\lambda_j^2\beta_j}\right]^{\mu_j}\right\}\right\} /\partial\lambda_j}{\left\{1-\overline{\alpha_J}\exp\left\{-\left[\frac{t_{ji}^2}{\lambda_j^2\beta_j}\right]^{\mu_j}\right\}\right\}} = 0 \tag{26}$$

and

$$\frac{\partial \log L_j(t_{ji},\ \alpha_j,\ \beta_j\lambda_j,\ \mu_j)}{\partial \mu_j} = -2n\log(\lambda_j) - n\log(\beta_j) + \frac{n}{\mu_j} - \sum_{i=1}^{n}\left[\frac{t_{ji}^2}{\lambda_j^2\beta_j}\right]$$

$$- \frac{2\sum_{i=1}^{n}\log\left\{1-\overline{\alpha_J}\exp\left\{-\left[\frac{t_{ji}^2}{\lambda_j^2\beta_j}\right]^{\mu_j}\right\}\right\} /\partial\mu_j}{\left\{1-\overline{\alpha_J}\exp\left\{-\left[\frac{t_{ji}^2}{\lambda_j^2\beta_j}\right]^{\mu_j}\right\}\right\}} = 0 \tag{27}$$

Solving the system of nonlinear Equations (24)-(27) yields the Maximum Likelihood Estimates (MLEs) for the parameters $\alpha_j,\ \beta_j,\ \lambda_j$, and μ_j.

To ensure the existence of maximum likelihood estimators, regularity conditions were imposed. Under the observed data conditions, the likelihood function demonstrated well-behaved characteristics, resulting in unique and finite MLEs. Additionally, numerical checks were performed to verify the convergence and stability of the estimates. Specifically, multiple starting points were utilized, and consistent convergence was observed.

4.1.2 *Two-stage estimation*

This paper proposes a method that begins by estimating the parameters of the marginal distributions F_1 and F_2 independently using MLE, as given below:

$$\log L_j = \sum_{i=1}^{n}\log f_j(x_{ji}), \quad j = 1,\ 2. \tag{28}$$

The MLEs for $\alpha_j,\ \beta_j,\ \lambda_j$ and μ_j can be obtained by setting Equations (24)-(27) to zero. These equations typically require numerical methods to solve the equations. Iterative techniques, such as a Newton-Raphson type algorithm, can be employed to obtain these estimates. Following this, the second step involves estimating the copula parameter θ by maximizing the copula density, as shown below.

$$\log L(\theta) = \sum_{i=1}^{n} \log\left[c_\theta(\widehat{U}_i,\ \widehat{V}_i)\right], \tag{29}$$

where $\widehat{U}_i,\ \widehat{V}_i$ represent pseudo-observations, calculated from $\widehat{U}_i = \dfrac{R_{1i}}{n+1} = \dfrac{n}{n+1}\widehat{F}_1(t_{1i})$, $\widehat{V}_i = \dfrac{R_{2i}}{n+1} = \dfrac{n}{n+1}\widehat{F}_1(t_{2i})$, and $R_{1i},\ R_{2i}$ are, respectively, the ranks of $t_{1i},\ t_{2i}$.

It's crucial to note that the marginal CDFs are estimated parametrically in the initial step. Applying the invariance property of the maximum likelihood estimators, one can obtain the estimators for the RF and HRF by substituting the parameter estimates with their corresponding MLE $(\widehat{\alpha}_j,\ \widehat{\beta}_J,\ \widehat{\lambda}_J,\ \widehat{\mu}_J,\ \widehat{\theta})$ values in Equations (10) and (11).

Then

$$\begin{aligned}
\widehat{R}(t_1,\ t_2) &= 1 - C(F_1(t_1),\ F_2(t_2)) \\
&= 1 - \prod_{j=1}^{2} \frac{\dfrac{\widehat{\alpha}_j\widehat{\mu}_J g(y_{j(s)},\ \widehat{\lambda}_J)}{\widehat{\beta}_J 1 - G(y_{j(s)},\ \widehat{\lambda}_J)} \left\{ -\dfrac{\log[1 - G(y_{j(s)},\ \widehat{\lambda}_J)]}{\widehat{\beta}_J} \right\}^{\widehat{\mu}_J - 1} \exp\left\{ -\left[-\dfrac{\log[1 - G(y_{j(s)},\ \widehat{\lambda}_J)]}{\widehat{\beta}_J} \right]^{\widehat{\mu}_J} \right\}}{\left\{ 1 - \widehat{\widehat{\alpha}}_J \exp\left\{ -\left[-\dfrac{\log[1 - G(y_{j(s)},\ \widehat{\lambda}_J)]}{\widehat{\beta}_J} \right]^{\widehat{\mu}_J} \right\} \right\}^2} \\
&\quad \times c(F_1(y_{1(s)}),\ F_2(y_{2(s)}))
\end{aligned} \tag{30}$$

and

$$\hat{h}(t_1,\ t_2) = \frac{f(t_1,\ t_2,\ \widehat{\alpha}_j,\ \widehat{\beta}_J,\ \widehat{\lambda}_J,\ \widehat{\mu}_J,\ \widehat{\theta})}{R(t_1,\ t_2,\ \widehat{\alpha}_j,\ \widehat{\beta}_J,\ \widehat{\lambda}_J,\ \widehat{\mu}_J,\ \widehat{\theta})}, \tag{31}$$

$$\hat{h}(t_1,\ t_2) = \frac{\prod_{j=1}^{2} \frac{\widehat{\alpha}_j\widehat{\mu}_J}{\widehat{\beta}_J} \frac{g(t_j,\ \widehat{\lambda}_J)}{1 - G(t_j,\ \widehat{\lambda}_J)} \left\{ -\frac{\log[1 - G(t_j,\ \widehat{\lambda}_J)]}{\widehat{\beta}_J} \right\}^{\widehat{\mu}_J - 1} \exp\left\{ -\left[-\frac{\log[1 - G(t_j,\ \widehat{\lambda}_J)]}{\widehat{\beta}_J} \right]^{\widehat{\mu}_J} \right\}}{\left\{ 1 - \widehat{\widehat{\alpha}}_J \exp\left\{ -\left[-\frac{\log[1 - G(t_j,\ \widehat{\lambda}_J)]}{\widehat{\beta}_J} \right]^{\widehat{\mu}_J} \right) \right\}^2} \times c\left(F_1(t_1),\ F_2(t_2)\right)}{1 - C\left(F_1(t_1),\ F_2(t_2)\right)} \tag{32}$$

$\widehat{R}(t_1,\ t_2)$ and $\hat{h}(t_1,\ t_2)$ can be evaluated numerically.

4.2 *Maximum likelihood prediction*

Two-sample prediction assumes that the two datasets are independent and originate from the same underlying distribution. For the univariate distributions, the predictive PDF for the s-th order statistic in a future sample is

derived using its density. For bivariate Type II censoring, where the first component of the vector represents the ordered observation and the second is its concomitant, obtaining the joint predictive density function for future ordered observations and their concomitants requires the joint PDF of the ordered observations and their concomitants.

For a future bivariate censored sample of size m, the joint pdf of the future s-th ordered observation and its s-th concomitant denoted by $(y_{1(s:m)},\, y_{2(s:m)})$, $s = 1,\, 2,\, \ldots,\, m$ has the joint pdf which is given by (9) after replacing t_1 with $y_{1(s:m)}$ and t_2 with $y_{2(s:m)}$. For simplicity, it can be written as $(y_{1(s)},\, y_{2(s)})$ for $(y_{1(s:m)},\, y_{2(s:m)})$, (for more details, see [33–37]). Then the joint PDF of $(y_{1(s)},\, y_{2(s)})$ is given by

$$f_{s:m}(y_{1(s)},\, y_{2(s)};\, \underline{\omega}) = \frac{m!}{(s-1)!(m-s)!} f(y_{1(s)},\, y_{2(s)};\, \underline{\omega})[F(y_{1(s)},\, y_{2(s)})]^{s-1} \times [1 - F(y_{1(s)},\, y_{2(s)})]^{m-s} \tag{33}$$

Applying the binomial expansion to simplify the last term of the preceding equation yields:

$$[1 - F(y_{1(s)},\, y_{2(s)})]^{m-s} = \sum_{r=0}^{m-s} \binom{m-s}{r} (-1)^r [F(y_{1(s)},\, y_{2(s)})]^r \tag{34}$$

Thus, the joint PDF of $(y_{1(s)},\, y_{2(s)})$ is

$$\begin{aligned} f_{s:m}(y_{1(s)},\, y_{2(s)};\, \underline{\omega}) &= \frac{m!}{(s-1)!(m-s)!} f(y_{1(s)},\, y_{2(s)};\, \underline{\omega}) \sum_{r=0}^{m-s} \binom{m-s}{r} (-1)^r [F(y_{1(s)},\, y_{2(s)})]^{s+r-1}, \\ &= f(y_{1(s)},\, y_{2(s)};\, \underline{\omega}) \sum_{r=0}^{m-s} \frac{m!}{(s-1)!(m-s-r)!(r)!} (-1)^r [F(y_{1(s)},\, y_{2(s)})]^{s+r-1}, \\ &= f(y_{1(s)},\, y_{2(s)};\, \underline{\omega}) \sum_{r=0}^{m-s} C_{m,\, s,\, r} [F(y_{1(s)},\, y_{2(s)})]^{s+r-1} \end{aligned} \tag{35}$$

where

$$C_{m,\, s,\, r} = \frac{m!}{(s-1)!(m-s-r)!(j)!} (-1)^r \tag{36}$$

Substituting the expressions for $F(t_1,\, t_2)$ and $f(t_1,\, t_2)$ given in (12) and (16), respectively, replacing t_1 with $y_{1(s)}$ and t_2 with $y_{2(s)}$, the joint MLE predictive density of the ordered observations and their concomitants is obtained as follows:

$$f_{s:m}(y_{1(s)},\, y_{2(s)};\, \widehat{\alpha}_j,\, \widehat{\beta}_J,\, \widehat{\lambda}_J,\, \widehat{\mu}_J,\, \widehat{\theta})$$

$$= \prod_{j=1}^{2} \frac{\frac{\widehat{\alpha}_j \widehat{\mu}_J}{\widehat{\beta}_J} \frac{g\left(y_{j(s)},\, \widehat{\lambda}_J\right)}{1-G\left(y_{j(s)},\, \widehat{\lambda}_J\right)} \left\{ -\frac{\log\left[1-G\left(y_{j(s)},\, \widehat{\lambda}_J\right)\right]}{\widehat{\beta}_J} \right\}^{\widehat{\mu}_J-1} \exp\left\{ -\left[-\frac{\log\left[1-G\left(y_{j(s)},\, \widehat{\lambda}_J\right)\right]}{\widehat{\beta}_J} \right]^{\widehat{\mu}_J} \right\}}{\left\{ 1-\widehat{\overline{\alpha}_J} \exp\left\{ -\left[-\frac{\log\left[1-G\left(y_{j(s)},\, \widehat{\lambda}_J\right)\right]}{\widehat{\beta}_J} \right]^{\widehat{\mu}_J} \right\} \right\}^2} \tag{37}$$

$$\times c(F_1(y_{1(s)}),\, F_2(y_{2(s)})) \sum_{r=0}^{m-s} C_{m,\, s,\, r} \left\{ C(F_1(y_{1(s)}),\, F_2(y_{2(s)})) \right\}^{(s+r-1)},$$

$$(y_{1(s)},\, y_{2(s)}) > 0,\, (\widehat{\alpha}_j,\, \widehat{\beta}_J,\, \widehat{\lambda}_J,\, \widehat{\mu}_J,\, \widehat{\theta}) > 0.$$

The point predictors of future ordered observation and their concomitants $(Y_{1(s)},\, Y_{2(s)})$, $s = 1,\, 2,\, \ldots,\, m$, can be obtained as follows:

$$\widehat{Y}_1 = E(y_{1(s)};\, \underline{\widehat{\omega}}_{ML}) = \int_{y_{1(s)}=0}^{\infty} y_{1(s)} \int_{y_{2(s)}}^{\infty} f(y_{1(s)},\, y_{2(s)};\, \underline{\widehat{\omega}}_{ML}) dy_{2(s)} dy_{1(s)}, \tag{38}$$

$$\widehat{Y}_2 = E(y_{2(s)};\, \underline{\widehat{\omega}}_{ML}) = \int_{y_{2(s)}=0}^{\infty} y_{2(s)} \int_{y_{1(s)}}^{\infty} f(y_{1(s)},\, y_{2(s)};\, \underline{\widehat{\omega}}_{ML}) dy_{1(s)} dy_{2(s)}, \tag{39}$$

The joint point predictors of the future ordered observation is

$$\widehat{Y}_1,\, \widehat{Y}_2 = E(y_{1(s)},\, y_{2(s)};\, \underline{\widehat{\omega}}_{ML}) = \int_0^{\infty} \int_0^{\infty} y_{1(s)} y_{2(s)} f(y_{1(s)},\, y_{2(s)};\, \underline{\widehat{\omega}}_{ML}) dy_{2(s)} dy_{1(s)}, \tag{40}$$

which can be evaluated numerically.

5. Goodness of fit tests for copula

The core concept of this test is to assess how well a specific parametric copula, denoted as C, represents the empirical copula derived from the data. This comparison is made under the assumption of the null hypothesis, as detailed in [25, 39].

$$H_0 : C = C_\theta \quad \text{Vs.} \quad H_1 : C \neq C_\theta \tag{41}$$

where C_θ is a specific copula.

In the literature, two primary methods are frequently employed to assess how well a copula fits the data: the parametric bootstrap, as described in [25], and the fast multiplier approach, detailed in [25, 39].

Goodness-of-fit tests based on the empirical process are widely used in the literature and offer a powerful framework for copula validation.

$$C_n(u,\ v) = \sqrt{n}\left\{C_n(u,\ v) - C_{\theta_n}(u,\ v)\right\}, \tag{42}$$

where $C_n(u,\ v)$ is the empirical copula of the data of T_1 and T_2.

$$C_n(u,\ v) = \frac{1}{n}\sum_{i=1}^{n} 1(U_{i,\ n} \le u,\ V_{i,\ n} \le v), \quad u,\ v \in [0,\ 1], \tag{43}$$

where $U_{i,\ n},\ V_{i,\ n}$ are pseudo-observations from C calculated from data are as follows:

$U_{i,\ n} = \dfrac{R_{1i}}{n+1}$, $V_{i,\ n} = \dfrac{R_{2i}}{n+1}$, and $R_{1i},\ R_{2i}$ are respectively the ranks of $t_{1i},\ t_{2i},$ where $C_n(u,\ v)$ is a consistent estimator and θ_n is an estimator of θ obtained using the pseudo-observations. According to [24], the test statistics is the Cramér-von Miss and is defined as

$$S_n = \sum_{i=1}^{n}\left\{C_n(U_{i,\ n},\ V_{i,\ n}) - C_{\theta_n}(U_{i,\ n},\ V_{i,\ n})\right\}^2. \tag{44}$$

Readers interested in a more detailed explanation are encouraged to refer to [33, 39–42].

6. Numerical illustration

This section employs a Monte Carlo simulation to compare the performance of different estimation methods based on the FGM copula, specifically MLE and TSE, when estimating the parameters of the FGM-BMOWR distribution. The simulations were conducted using Mathematica 11 and the R programming language.

To generate random variables from a specific joint distribution, the conditional distribution method is utilized, as introduced by [38]. The joint distribution function is given by:

$$f(x_1,\ x_2) = f(x_1)f(x_2 \mid x_1). \tag{45}$$

To compare the performance of the MLE and TSE methods, the biases, Estimated Risk (ER), Relative Absolute Biases (RAB), Standard Errors (SE), and Confidence Intervals (CIs) are used as comparison criteria, considering various sample sizes. For each sample size (n) and a set of specified parameter values, 5,000 datasets are generated from the FGM-BMOWR distribution with the following parameter values:

Case I: $(\theta = 0.01,\ \alpha_1 = 0.8,\ \alpha_2 = 0.9,\ \beta_1 = 0.9,\ \beta_2 = 0.8,\ \mu_1 = 0.4,\ \mu_2 = 0.8,\ \lambda_1 = 0.9,\ \lambda_2 = 0.8)$.

Case II: $(\theta = 0.7,\ \alpha_1 = 0.3,\ \alpha_2 = 0.9,\ \beta_1 = 0.4,\ \beta_2 = 0.5,\ \mu_1 = 0.8,\ \mu_2 = 0.4,\ \lambda_1 = 0.8,\ \lambda_2 = 0.9)$;

Sample sizes of 30, 50, and 100 are used to represent the small, medium, and large sample sizes commonly found in real-world datasets.

The steps involved in the simulation procedure are outlined below:

1. Generating random samples from an FGM-BMOWR distribution with a given parameter vector $\vartheta = (\theta,\ \alpha_1,\ \alpha_2,\ \beta_1,\ \beta_2\mu_1,\ \mu_2,\ \lambda_1,\ \lambda_2)$ for samples of size 30, 50, and 100.

2. For each sample size, the generated data are sorted to obtain the ordered values t_{ij}'s such that $(t_{11},\ t_{21}),\ (t_{12},\ t_{22}),\ \ldots,\ (t_{1n},\ t_{2n})$.

3. The preceding two steps are repeated N times, with N representing the total number of simulated samples.

4. The Newton-Raphson method can be used to calculate the averages of the Maximum Likelihood (ML) estimates and the CIs for the parameters.

5. The accuracy of the estimates is evaluated using several performance measures to assess the precision and variability of the estimates such as

$$ER = \frac{\sum_{j=1}^{N}(\widehat{\widehat{\vartheta}}_{i,\,j} - \theta_i)^2}{N}, \quad \text{Bias}(\widehat{\vartheta}_i) = \frac{\sum_{j=1}^{N}(\widehat{\widehat{\vartheta}}_{i,\,j} - \theta_i)}{N}, \quad i = 1,\, 2,\, ...,\, 9. \tag{46}$$

The chain is run for 5,000 iterations.

As expected, for both methods, the ERs, RABs, biases, and SEs are close to zero, and the CIs are close to the nominal value of 95%.

Tables 1 and 2 present the averages of the ML estimates, ERs, RABs, biases, SEs, and CIs for the unknown parameters. Similarly, Tables 3 and 4 provide the TSE averages, ERs, RABs, biases, SEs, and CIs for the unknown parameters. Tables 1 and 3 correspond to Case I, while Tables 2 and 4 relate to Case II. The MLE two-sample predictors are shown in Table 5.

Table 1. ML averages, estimated risks, relative absolute biases, biases, squared errors, and 95% confidence intervals of the parameters (Case I) ($\theta = -0.01,\ \alpha_1 = 0.8,\ \alpha_2 = 0.9,\ \beta_1 = 0.9,\ \beta_2 = 0.8,\ \mu_1 = 0.8,\ \mu_2 = 0.4,\ \lambda_1 = 0.9,\ \lambda_2 = 0.8$)

n	Parameters	Averages	ER	RAB	bias	SE	UL	LL	Length
30	θ	−0.1878	0.3087	−0.7316	0.2622	0.4898	0.7727	−1.1480	1.9203
	α_1	0.8472	0.0043	0.0590	0.0022	0.0660	0.9768	0.7177	0.2591
	α_2	0.6765	0.0819	0.2482	0.0499	0.2819	1.2291	0.1239	1.1052
	β_1	0.9878	0.3562	1.4697	0.34560	0.4866	1.94171	0.03400	1.9077
	β_2	0.8983	0.1727	0.7966	0.1586	0.3840	1.6511	0.1455	1.5056
	μ_1	0.5535	0.0956	0.3080	0.0607	0.3032	1.1479	0.0000	1.1479
	μ_2	0.8944	0.2576	1.2360	0.2444	0.4448	1.7664	0.0224	1.7439
	λ_1	0.9878	0.0459	0.2348	0.353	0.2115	1.4024	0.5733	0.8291
	λ_2	0.7665	0.0303	0.14827	0.0178	0.17310	1.1059	0.42714	0.6788
50	θ	−0.1964	0.3018	−0.7194	0.2536	0.4873	0.7588	−1.1516	1.9105
	α_1	0.8352	0.0030	0.0440	0.0012	0.0553	0.9437	0.7267	0.2170
	α_2	0.9265	0.0209	0.0294	0.0007	0.1448	1.2105	0.6425	0.5679
	β_1	0.9212	0.2728	1.3030	0.2716	0.4461	1.7596	0.0467	1.7489
	β_2	0.7679	0.0749	0.5359	0.0718	0.2641	1.2857	0.2502	1.0354
	μ_1	0.4721	0.1103	0.4098	0.1075	0.3142	1.0881	0.0000	1.0881
	μ_2	0.7578	0.1332	0.8946	0.1280	0.3418	1.4278	0.0878	1.3400
	λ_1	0.9212	0.0158	0.1515	0.0146	0.1252	1.1666	0.6757	0.4908
	λ_2	0.7679	0.0205	0.1467	0.0174	0.1423	1.0468	0.4890	0.5578
100	θ	−0.3274	0.1581	−0.5321	0.1387	0.3726	0.4029	−1.0579	1.4608
	α_1	0.8272	0.0009	0.0340	0.0007	0.0302	0.8864	0.76801	0.1184
	α_2	0.8855	0.0105	0.1609	0.0002	0.1026	1.9338	0.6843	0.4022
	β_1	0.9104	0.2606	1.2760	0.2605	0.4391	1.7710	0.0497	1.7212
	β_2	0.7274	0.06012	0.4549	0.0517	0.2396	1.1972	0.2577	0.9395
	μ_1	0.4841	0.1009	0.3948	0.0997	0.3017	1.0755	0.0000	1.0755
	μ_2	0.6912	0.0965	0.7281	0.0848	0.2989	1.2771	0.1053	1.1717
	λ_1	0.9104	0.0123	0.1380	0.0121	0.1104	1.1269	0.6939	0.4330
	λ_2	0.8127	0.0201	0.0969	0.0076	0.1415	1.0902	0.5351	0.5550

Table 2. ML averages, estimated risks, relative absolute biases, biases, squared errors, and 95% confidence intervals of the parameters (Case II) ($\theta = 0.7$, $\alpha_1 = 0.3$, $\alpha_2 = 0.9$, $\beta_1 = 0.4$, $\beta_2 = 0.5$, $\mu_1 = 0.8$, $\mu_2 = 0.4$, $\lambda_1 = 0.8$, $\lambda_2 = 0.9$)

n	Parameters	Averages	ER	RAB	bias	SE	UL	LL	Length
30	θ	1.1616	0.2131	0.6595	0.2131	0.4095	1.9643	0.3590	1.6053
	α_1	0.2521	0.0137	0.1594	0.0022	0.1170	0.4816	0.0226	0.4590
	α_2	1.4295	0.2846	0.5883	0.2804	0.4539	2.319	0.5398	1.7793
	β_1	0.5371	0.0374	0.3428	0.0188	0.1925	0.9144	0.1598	0.7546
	β_2	0.6794	0.0469	0.3588	0.0321	0.2143	1.0995	0.2592	0.8402
	μ_1	1.1038	0.2321	0.3798	0.0923	0.4728	2.0306	0.1770	1.8535
	μ_2	0.4954	0.0175	0.2385	0.0091	0.1320	0.7541	0.2366	0.5174
	λ_1	1.07425	0.1496	0.3428	0.0752	0.3794	1.8179	0.3305	1.4874
	λ_2	1.2229	0.1522	0.3588	0.1042	0.3759	1.9598	0.4860	1.4737
50	θ	1.1125	0.1701	0.5892	0.1702	0.3757	1.8490	0.3759	1.4730
	α_1	0.2843	0.0086	0.0521	0.0002	0.0927	0.4662	0.1025	0.3636
	α_2	1.12279	0.0923	0.2532	0.0519	0.2994	1.7148	0.5410	1.1737
	β_1	0.4372	0.0091	0.0930	0.0013	0.0954	0.6242	0.2501	0.3740
	β_2	0.5380	0.0025	0.0761	0.0014	0.0508	0.6377	0.4384	0.1992
	μ_1	0.8912	0.0978	0.1140	0.0083	0.3127	1.5042	0.2781	1.0060
	μ_2	0.4138	0.0012	0.0345	0.0002	0.0357	0.4839	0.3437	0.1401
	λ_1	0.8744	0.0364	0.0930	0.0055	0.1907	1.2483	0.5004	0.7478
	λ_2	0.9685	0.0083	0.0761	0.0047	0.0914	1.1477	0.7894	0.3583
100	θ	1.1007	0.1605	0.5724	0.1605	0.3671	1.8203	0.3811	1.4391
	α_1	0.3379	0.0023	0.1263	0.0014	0.0484	0.4329	0.2428	0.1900
	α_2	0.9919	0.0178	0.1021	0.0084	0.1334	1.253	0.7304	0.5229
	β_1	0.3832	0.0006	0.0419	0.0003	0.0262	0.4347	0.3316	0.1030
	β_2	0.5140	0.0003	0.0281	0.0002	0.0180	0.5494	0.4786	0.0708
	μ_1	0.7215	0.0011	0.0980	0.0061	0.1066	0.9306	0.5125	0.4180
	μ_2	0.4041	0.0001	0.0104	1.7490e-5	0.0137	0.4311	0.3772	0.0539
	λ_1	0.7664	0.0027	0.0419	0.0011	0.52.5	0.8694	0.6633	0.2061
	λ_2	0.9253	0.0010	0.0281	0.0006	0.0325	0.9890	0.8615	0.1275

Table 3. TSE averages, estimated risks, relative absolute biases, biases, squared errors, and 95% confidence intervals of the parameters (Case II) ($\theta = 0.7$, $\alpha_1 = 0.3$, $\alpha_2 = 0.9$, $\beta_1 = 0.4$, $\beta_2 = 0.5$, $\mu_1 = 0.8$, $\mu_2 = 0.4$, $\lambda_1 = 0.8$, $\lambda_2 = 0.9$)

n	Parameters	Averages	ER	RAB	bias	SE	UL	LL	Length
30	θ	0.5394	0.0051	0.2294	0.0257	0.3934	1.3105	−0.2317	1.5422
	α_1	0.3905	0.0008	0.3019	0.0082	0.1989	0.7804	0.0007	0.7798
	α_2	0.6704	0.0105	0.2550	0.0526	0.3947	1.4442	0.0000	1.4442
	β_1	0.5429	0.0040	0.357.	0.0204	0.1757	0.8873	0.1985	0.6887
	β_2	0.5475	0.0005	0.0951	0.0022	0.1891	0.9182	0.1769	0.7412
	μ_1	1.0217	0.0049	0.2771	0.0491	0.6793	2.3533	0.0000	2.3533
	μ_2	0.4245	0.0001	0.061	0.0006	0.0305	0.4844	0.3646	0.1198
	λ_1	1.0858	0.0163	0.3573	0.0817	0.3442	1.7605	0.4112	1.3493
	λ_2	1.1888	0.0166	0.3209	0.0834	0.2791	1.7359	0.6417	1.0941
50	θ	0.7831	0.0004	0.1188	0.0069	0.3640	1.4966	0.0696	1.4269
	α_1	0.3608	0.0007	0.2028	0.0037	0.1624	0.6792	0.0424	0.6368
	α_2	0.8497	0.0002	0.0558	0.0025	0.3181	1.4732	0.2262	1.2470
	β_1	0.4650	0.0008	0.1626	0.0042	0.1692	0.7967	0.1333	0.6633
	β_2	0.5365	0.0001	0.0730	0.0013	0.1690	0.8677	0.2052	0.6625
	μ_1	0.9627	0.0026	0.2034	0.0264	0.4620	1.8684	0.0571	1.8113
	μ_2	0.4090	5.4552e-6	0.0226	0.0001	0.0210	0.4502	0.3678	0.0824
	λ_1	0.9491	0.0022	0.1864	0.0222	0.3066	1.5502	0.3480	1.2022
	λ_2	1.0965	0.0025	0.2184	0.0386	0.2455	1.5779	0.6152	0.9626
100	θ	0.6869	3.3810e-5	0.01857	0.0001	0.2191	1.1165	0.2574	0.8591
	α_1	0.3014	4.2274e-7	0.0048	2.1137e-6	0.1138	0.5245	0.0783	0.4462
	α_2	0.86751	0.0002	0.0360	0.0010	0.2874	1.430	0.3040	1.1269
	β_1	0.4290	0.0001	0.0726	0.0008	0.1124	0.6494	0.2086	0.4407
	β_2	0.5103	2.1380e-5	0.0206	0.0001	0.1533	0.8109	0.2097	0.6012
	μ_1	0.8569	0.0006	0.0711	0.0032	0.3824	1.6066	0.1072	1.4993
	μ_2	0.4046	4.3224e-6	0.0116	2.1611e-5	0.0164	0.4368	0.3724	0.0644
	λ_1	0.8581	0.0006	0.0726	0.0034	0.2248	1.2988	0.4174	0.8814
	λ_2	0.9470	0.0004	0.0523	0.0022	0.0543	1.0536	0.8404	0.2131

Table 4. TSE averages, estimated risks, relative absolute biases, biases, squared errors, and 95% confidence intervals of the parameters (Case II)

n	Parameters	Averages	ER	RAB	bias	SE	UL	LL	Length
30	θ	0.0051	0.00004	0.4899	0.00002	0.0066	0.0078	0.0000	0.0259
	α_1	0.9407	0.0439	0.1759	0.0198	0.2086	1.3497	0.5318	0.8178
	α_2	1.1306	0.0885	0.2562	0.0531	0.2927	1.7043	0.5568	1.1474
	β_1	0.8656	0.0311	0.0381	0.0011	0.1764	1.2115	0.5197	0.6918
	β_2	1.2691	0.3735	0.5864	0.2201	0.5702	2.3866	0.1517	2.2350
	μ_1	0.5381	0.0299	0.3452	0.0191	0.1720	0.8752	0.2009	0.6743
	μ_2	0.8411	0.0188	0.0514	0.0017	0.1373	1.1103	0.5719	0.5382
	λ_1	0.8656	0.0311	0.0381	0.0012	0.1764	1.2115	0.5197	0.6918
	λ_2	0.8291	0.0017	0.0367	0.0008	0.0414	0.9103	0.7478	0.1624
50	θ	0.0068	0.00003	0.3170	0.00001	0.0043	0.0018	0.0000	0.0171
	α_1	0.9251	0.02499	0.1563	0.01564	0.1573	1.2334	0.6167	0.6166
	α_2	0.9981	0.0425	0.1089	0.0096	0.2061	1.4020	0.5941	0.8079
	β_1	0.8131	0.0162	0.0965	0.0075	0.1271	1.0623	0.5638	0.4984
	β_2	0.0223	0.2244	0.2778	0.0493	0.4711	1.9457	0.0987	1.8469
	μ_1	0.4576	0.0084	0.1442	0.0033	0.0916	0.6373	0.2779	0.3593
	μ_2	0.7849	0.0061	0.0188	0.0002	0.0782	0.9384	0.6314	0.3069
	λ_1	0.8131	0.0162	0.0965	0.0075	0.1271	1.0623	0.5638	0.4984
	λ_2	0.8143	0.0009	0.0179	0.0002	0.0307	0.8744	0.7542	0.1202
100	θ	0.0073	0.00001	0.2617	6.8506e-6	0.0039	0.0002	0.0000	0.0153
	α_1	0.9077	0.0235	0.1347	0.0116	0.1530	1.2077	0.6077	0.6000
	α_2	0.9895	0.0335	0.0994	0.0080	0.1830	1.3483	0.6306	0.7177
	β_1	0.8266	0.0123	0.0814	0.0053	0.1111	1.0446	0.6087	0.4358
	β_2	0.9878	0.1457	0.2347	0.0532	0.3801	1.7328	0.2427	1.49009
	μ_1	0.4570	0.0095	0.1427	0.0032	0.0976	0.6484	0.26577	0.3826
	μ_2	0.8271	0.0029	0.0339	0.0007	0.0541	0.9333	0.7210	0.2123
	λ_1	0.8266	0.0123	0.0814	0.0053	0.1111	1.0446	0.6087	0.4358
	λ_2	0.8124	0.0006	0.0155	0.0001	0.0261	0.8636	0.7612	0.1023

Table 5. ML predictive, and bounds of future observations under two-sample prediction ($\theta = 0.01,\ \alpha_1 = 0.8,\ \alpha_2 = 0.9,\ \beta_1 = 0.9,\ \beta_2 = 0.8,\ \mu_1 = 0.4,\ \mu_2 = 0.8,\ \lambda_1 = 0.9,\ \lambda_2 = 0.8$)

n	s	$y(s)$	Predictor	UL	LL	Length
30	4	$y_1(s)$	1.2033	3.8941	0.2946	3.5994
		$y_2(s)$	1.2953	1.7309	0.5682	1.1627
	5	$y_1(s)$	3.4844	7.5192	2.5783	4.9409
		$y_2(s)$	1.8099	6.4600	0.3397	6.1202
	6	$y_1(s)$	5.7470	8.3553	2.0862	6.2691
		$y_2(s)$	5.5945	12.0386	1.8813	10.1573

From the tables, one can conclude the following:

1. Tables 1-4 demonstrate that as the sample size increases, the averages obtained from both MLE and TSE converge towards the true population parameter values. Furthermore, the ER decreases with larger sample sizes. This indicates that the accuracy of the estimates improves, and they become better approximations of the true population parameter values as more data become available.

2. As the sample size increases, the CIs for the parameters become shorter.

3. According to Table 5, the CI for predicting the first future observation (using MLE) is narrower than the CI for predicting the last future observation.

4. The CI obtained using MLE is shorter than that obtained using TSE.

5. The ER associated with MLE is smaller than that associated with TSE.

7. Real data analysis

This section aims to demonstrate the practical use of the FGM-BMOWR distribution by applying it to two real-world datasets. Our goal is to thoroughly evaluate how well the FGM-BMOWR distribution fits these datasets and compare its performance with existing distributions. Several measures are used to assess the goodness of fit including the Kolmogorov-Smirnov (K-S) statistic and its p-value, along with information criteria such as the AIC, the Corrected Akaike Information Criterion (CAIC), the BIC, and the Hannan-Quinn Information Criterion (HQIC). Lower values of these criteria indicate a better fit. By calculating these statistics for the fitted models, one can quantitatively compare their performance with the best-fitting model having the lowest values. This analysis will help us to determine the suitability of the FGM-BMOWR distribution for modeling these datasets and whether it surpasses other models used by previous researchers, ultimately highlighting its strengths in representing the data structure.

The FGM-BMOWR distribution, due to its ability to model dependent lifetime data, has potential applications in reliability engineering, particularly in systems with components that degrade over time and are subject to common shocks. It could be used to analyze the failure times of processor and memory components in computer systems, as demonstrated with the real dataset. Additionally, it could be applied in areas like financial risk assessment, where joint defaults of related assets are modeled, or in medical studies, to analyze the time-to-event data of correlated health outcomes.

7.1 *Application*

These data represent $n = 50$ simulated primitive computer series systems suggested by [31]. The dataset analyzed in this study comprises simulated data from 50 basic computer chain systems, with a particular focus on their processor and memory. The proper functioning of both components is essential for the computer's operation. The simulation assumes these systems experience rapid degradation over a short period (in hours), making them highly vulnerable to shocks. Such shocks can cause the processor, memory, or both components to fail simultaneously. Therefore, assuming independent failures of the processor and memory would be unrealistic, as a single catastrophic event can affect both. To accurately account for this inherent dependence between the failure times of these two components, the FGM copula model is utilized. The dataset is presented below:

Processor lifetime (X_1): 1.3640, 1.9292, 1.0051, 3.6621, 1.0986, 3.6621, 1.5254, 3.6621, 1.1917, 1.0833, 2.5372, 1.0833, 2.5913, 0.3309, 0.5079, 0.3309, 0.7947, 0.5784, 0.6270, 0.5520, 5.7561, 1.9386, 5.7561, 2.1000, 0.9938, 0.9867, 0.1058, 0.9867, 0.1058, 1.3989, 1.7494, 2.3757, 0.9096, 3.5202, 1.6465, 2.3364, 5.0533, 0.8584, 0.1181, 4.3435, 3.3887, 1.1739, 0.4614, 1.3482, 0.1955, 3.0935, 0.8503, 2.1396, 0.1115, 1.3288.

Memory lifetime (X_2): 1.3640, 3.9291, 1.0051, 0.0026, 1.0986, 0.0026, 4.4088, 0.0026, 0.0801, 3.3059, 2.4923, 3.3059, 2.5913, 0.3309, 5.3535, 0.3309, 0.7947, 1.8795, 1.7289, 0.5520, 0.3212, 4.0043, 0.3212, 2.0513, 1.7689, 0.9867, 0.1058, 0.9867, 0.1058, 4.1268, 2.3643, 2.7953, 0.6214, 1.4095, 2.0197, 0.1624, 2.3238, 1.9556, 0.0884, 1.0001, 1.9796, 3.3857, 0.8584, 1.9705, 0.1955, 3.0935, 2.8578, 2.1548, 0.1115, 0.9689.

Although the computer data are sequential in nature, ideally necessitating a likelihood function that reflects this sequence, our analysis employed a different approach. We modeled the time to the first failure using continuous distribution. While this method is not limited to on-chain systems, it can still provide valuable information regarding the data.

The efficacy of the FGM-BMOWR model was evaluated through a comparison with relevant bivariate distributions such as Bivariate Compound Exponentiated Survival Function of the Beta (BCESF-beta) presented by [36], Bivariate Burr Type III (BBurr III) suggested by [32], Bivariate Compound Exponentiated Survival Function of the Lomax (BCESF-Lomax) presented by [33], and Bivariate Lomax (BLomax) provided by [36]. The motivation for this comparison lies in assessing the relative strengths of each model in capturing the underlying dependence structure and marginal characteristics of our specific datasets (X_1 and X_2), which represent [Processor lifetime and Memory lifetime]. This comparative approach validates the robust performance of the proposed FGM-BMOWR model.

The ML estimator of marginal parameters with Standard Error (SE), as well as different measures of goodness of fit such as AIC, BIC, HQIC, CAIC, and K-S statistics with P-values for all competitive models are provided in Tables 6

and 7. The probabilities from the classifier datasets show the marginal distributions of X_1 and X_2 in Figure 5. Figures 6-8 show the fitted PDFs, CDFs, and PP plots for the FGM-BMOWR model and other distributions.

Table 6. ML estimate with different measures of goodness of fit test of marginal distribution

Data	Parameter	Average	SE	K-S	*P*-value
X_1	θ	0.1191	0.1778	0.26	0.0681
	α_1	0.6626	0.3380		
	β_1	1.9275	1.7638		
	μ_1	0.8551	0.4617		
	λ_1	1.4456	0.6404		
X_2	θ	0.4977	0.0972	0.24	0.1122
	α_2	0.6348	0.2730		
	β_2	1.2430	0.3138		
	μ_2	1.0633	0.4963		
	λ_2	1.657	0.9583		

Table 7. Statistics measures for all models based on the first dataset

Models	Parameter	Average	SE	AIC	BIC	HQIC	CAIC
BMOWR	θ	−0.0506	0.406	19.1541	36.362	25.707	23.654
	α_1	1.5791	0.4883				
	α_2	1.4425	0.4557				
	β_1	0.97436	0.1688				
	β_2	1.1538	0.2455				
	μ_1	0.4153	0.0153				
	μ_2	0.2940	0.0059				
	λ_1	0.9713	0.02936				
	λ_2	1.1538	0.0602				
FGMWGP	θ	0.4149	0.2989	450.432	463.816	455.528	453.098
	α_1	0.7057	0.0938				
	α_2	0.596	0.2896				
	β_1	0.8063	0.0063				
	β_2	0.8132	0.0863				
	δ_1	0.9664	0.1642				
	δ_2	1.3181	0.3798				
BCESF-beta	k	0.2046	1.0957	234.203	242.611	238.893	237.856
	b	0.6867	23.6962				
	λ_1	1.0879	3.4571				
	λ_2	0.3995	0.3978				
	δ_1	1.9584	1.1201				
	δ_2	0.1997	0.9945				
BBurr III	k	2.7392	5.7227	278.388	280.181	279.988	237.856
	a	0.7712	1.0234				
	c_1	0.5846	0.0028				
	c_2	0.6739	0.5796				
BCESF-Lomax	a	0.9809	1.4173	487.127	495.534	491.816	490.779
	b	1.7997	4.0088				
	α_1	1.5167	0.0278				
	α_2	2.2331	0.1100				
	θ_1	1.9212	0.0447				
	θ_2	3.1467	0.2184				
BLomax	α	1.1621	0.0038	792.186	795.661	793.46	792.494
	α_1	1.2659	0.0547				
	α_2	1.4091	0.6255				

The results of this comparative analysis, as detailed in Tables 6 and 7, indicate that the proposed BCESF-beta distribution demonstrates superior performance compared to the other considered distributions based on the evaluated goodness-of-fit measures. This suggests that the FGM-BMOWR model offers a better fit to the data while maintaining a comparable level of complexity.

Tables 8 and 9 show the MLE and TSE estimates, along with their SEs, of the unknown parameters for the dataset based on the complete sample. Moreover, MLE predictive values and bounds for future observations under two-sample prediction for different cases are given in Table 10.

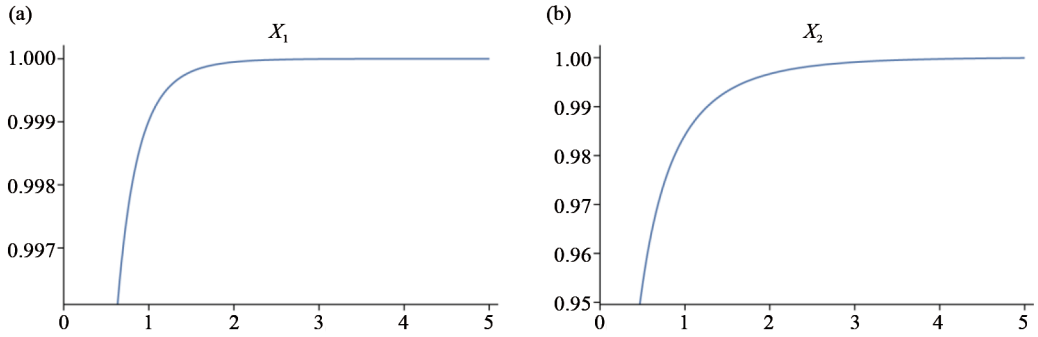

Figure 5. The probabilities from the classifier dataset showing the marginal distributions

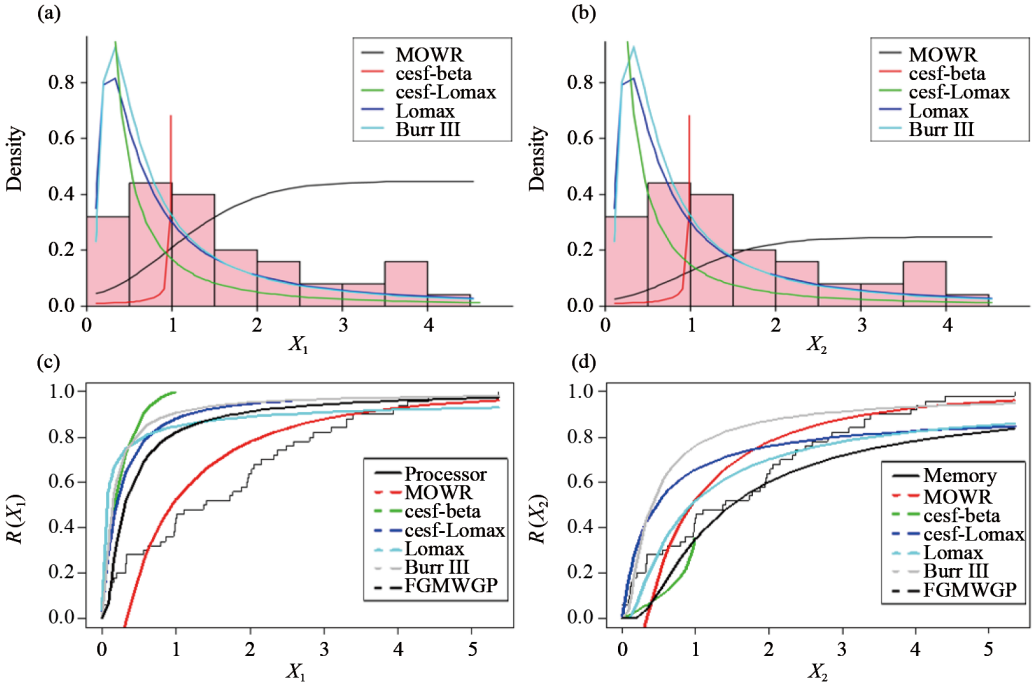

Figure 6. Estimated PDF and estimated distributions of the models for the dataset

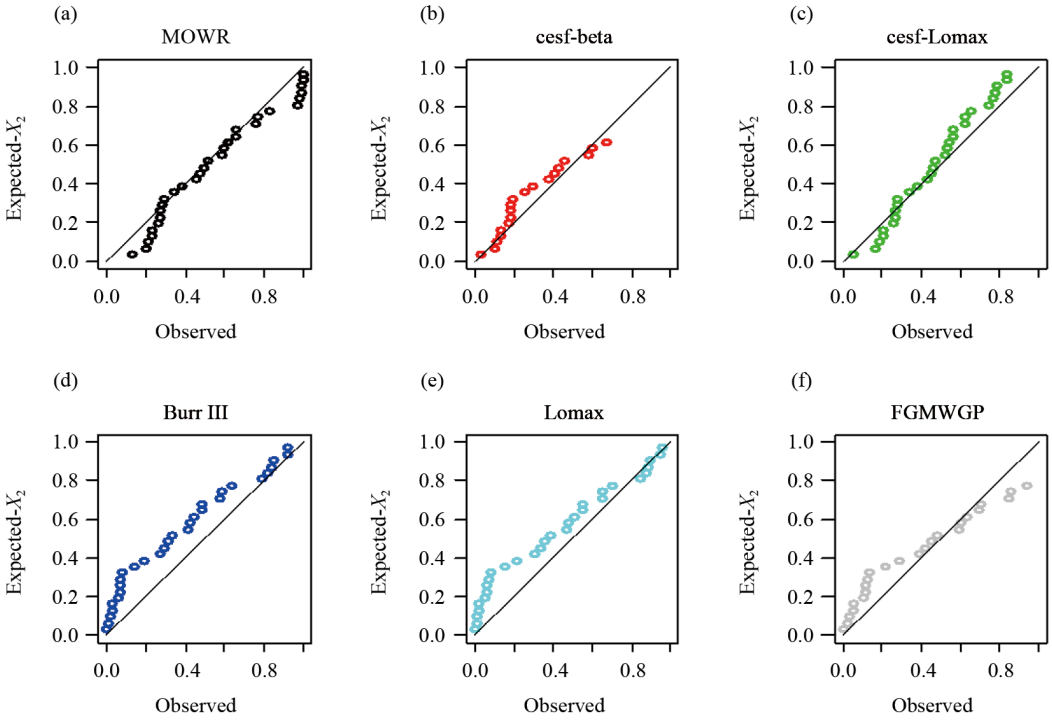

Figure 7. The PP plots of different models for the Dataset X_1

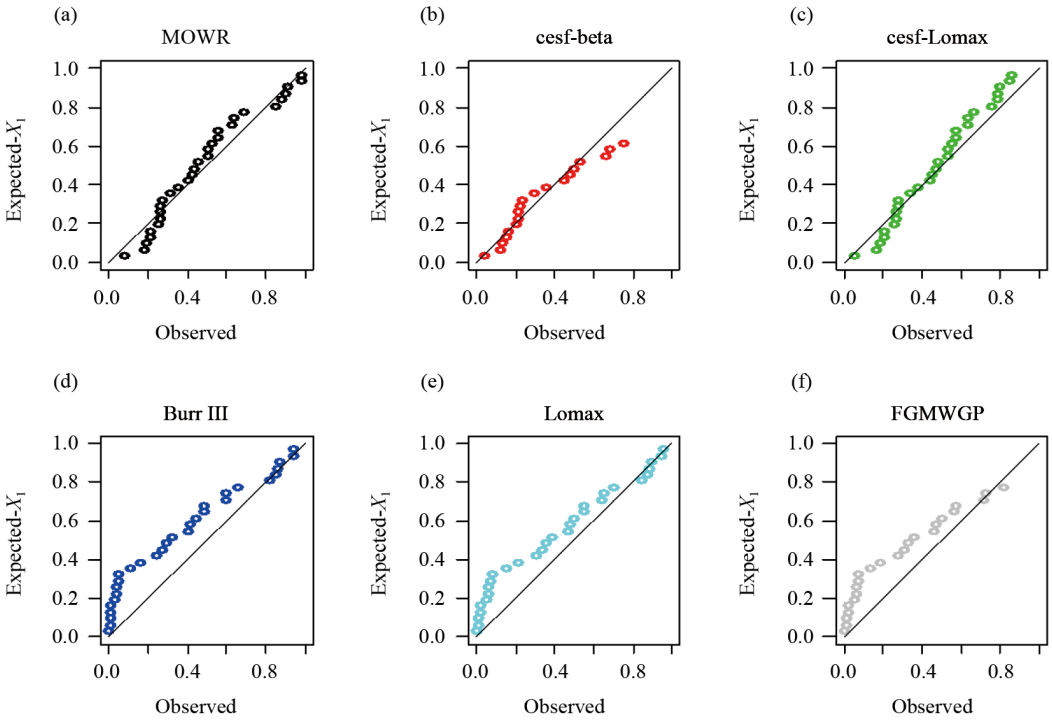

Figure 8. The PP plots of the different models for the Dataset X_2

Each plot in Figures 7 and 8 (MOWR, cesf-beta, cesf-Lomax, Burr III, and Lomax) represents a Q-Q plot comparing the empirical quantiles of our observed data X_1 and X_2, respectively, against the theoretical quantiles generated from the respective fitted distribution.

The MOWR plot in Figures 7 and 8 consistently shows points that are generally closer to a straight line compared to the other distributions (cesf-beta, cesf-Lomax, Burr III, and Lomax). This linearity indeed suggests that the MOWR distribution provides a better visual fit to the observed data than the others shown in Figures 7 and 8.

Table 8. MLE estimates, standard errors of the parameters (case I and case II)

n	Parameters	Estimate		SE	
		Case I	Case II	Case I	Case II
30	θ	−0.0506	0.5779	0.0406	0.1211
	α_1	1.5791	0.46565	0.4883	0.16336
	α_2	1.4425	1.4271	0.4557	0.4479
	β_1	0.9713	1.0373	0.1688	0.4911
	β_2	1.1538	1.064	0.2455	0.4657
	μ_1	0.4154	1.5677	0.0153	0.4919
	μ_2	0.2940	0.6005	0.0059	0.1964
	λ_1	0.9713	2.074	0.13688	1.0077
	λ_2	1.1538	1.9152	0.2455	0.1782

Table 9. TSE estimates, standard errors of the parameters (Case I and Case II)

n	Parameters	Estimate		SE	
		Case I	Case II	Case I	Case II
30	θ	0.0188	0.1978	0.0288	0.4343
	α_1	0.7797	0.5245	0.0202	0.2188
	α_2	1.2369	1.7609	0.3172	0.4379
	β_1	1.7206	0.5631	0.4689	0.1609
	β_2	3.9688	0.9044	0.0000	0.3698
	μ_1	0.7445	0.8911	0.1535	0.0907
	μ_2	0.5984	0.7421	0.1974	0.3214
	λ_1	1.7206	1.1262	0.0000	0.3083
	λ_2	1.4368	0.3755	0.4910	0.4465

Table 10. MLE predictive and bounds of future observations under two-sample prediction ($\theta = 0.01,\ \alpha_1 = 0.8,\ \alpha_2 = 0.9,\ \beta_1 = 0.9,\ \beta_2 = 0.8,\ \mu_1 = 0.4,\ \mu_2 = 0.8,\ \lambda_1 = 0.9,\ \lambda_2 = 0.8$)

n	s	$\widehat{y}_{(s)}$	Predictor	UL	LL	Length
50	10	$\widehat{y}_{1(s)}$	4.0085	7.1172	1.6491	5.4681
		$\widehat{y}_{2(s)}$	1.9612	2.9796	0.9212	2.0585
	11	$\widehat{y}_{1(s)}$	4.7821	7.3218	2.0926	5.2292
		$\widehat{y}_{2(s)}$	2.3167	3.0484	1.1576	1.8908
	12	$\widehat{y}_{1(s)}$	5.7025	7.5192	2.5783	4.9409
		$\widehat{y}_{2(s)}$	2.7317	3.1155	1.3824	1.7331

7.2 *Example dataset*

In this example, a dataset is analyzed from a Sankaran-Nair bivariate Pareto distribution (see [29, 37]). The generated dataset of $(X_1,\ X_2)$ for $n = 30$ is: (0.252, 8.400), (1.105, 0.458), (0.427, 1.602), (12.491, 2.383), (0.260, 0.106), (0.240,

1.769), (4.888, 0.758), (0.870, 0.572), (0.036, 0.254), (1.537, 0.023), (1.508, 0.535), (0.239, 1.4120), (0.173, 0.011), (1.090, 1.278), (6.002, 0.017), (0.897, 2.032), (0.690, 0.138), (1.883, 0.398), (0.960, 0.257), (0.561, 0.573), (5.370, 0.325), (0.167, 0.260), (13.602, 0.364), (3.922, 0.938), (0.132, 0.547), (0.603, 0.102), (0.226, 0.481), (0.143, 0.779), (0.643, 0.071), (0.349, 1.586).

Table 11. ML estimate with different measures of goodness of fit test of marginal distribution

Data	Parameter	Average	SE	K-S	P-value
X_1	θ	0.00010	0.0498	0.3333	0.7089
	α_1	0.1991	0.1491		
	β_1	0.8548	0.0895		
	μ_1	0.4482	0.4006		
	λ_1	1.3402	0.1388		
X_2	θ	0.0001	0.0697	0.3	0.135
	α_2	0.50360	0.0036		
	β_2	0.8516	0.0505		
	μ_2	0.4522	0.0302		
	λ_2	1.3818	0.0815		

Table 12. Statistics measures for all models based on the second dataset

Models	Parameter	Average	SE	AIC	BIC	HQIC	CAIC
BMOWR	θ	−4.686e-6	0.0099	18.0000	30.6108	27.0000	22.0343
	α_1	0.6881	0.1111				
	α_2	0.7784	0.1206				
	β_1	0.8127	0.0127				
	β_2	0.9397	0.0396				
	μ_1	0.4890	0.0887				
	μ_2	0.3597	0.0596				
	λ_1	0.8127	0.01270				
	λ_2	0.9397	0.3968				
BCESF-beta	k	0.2046	1.0957	234.203	242.611	238.893	237.856
	b	0.6867	23.6962				
	λ_1	1.0879	3.4571				
	λ_2	0.3995	0.3978				
	δ_1	1.9584	1.1201				
	δ_2	0.1997	0.9945				
BBurr III	k	2.7392	5.7227	278.388	283.992	280.181	279.988
	a	0.7712	1.0234				
	c_1	0.5846	0.0028				
	c_2	0.6739	0.5796				
BCESF-Lomax	a	0.9809	1.4173	487.127	495.534	491.816	490.779
	b	1.7997	4.0088				
	α_1	1.5167	0.0278				
	α_2	2.2331	0.1100				
	θ_1	1.9212	0.0447				
	θ_1	3.1467	0.2184				
BLomax	α	1.1621	0.0038	792.186	795.661	793.46	792.494
	α_1	1.2659	0.0547				
	α_2	1.4091	0.6255				

For this dataset, the FGM-BMOWR model will be compared against several other models: BCESF-beta, BBurr III, BCESF-Lomax [36], and BLomax [37]. The estimated parameters, SE for the data and these models, along with the AIC, CAIC, and HQIC statistics, are presented in Tables 11 and 12. Figure 8 displays the marginal distributions of X_1 from the classifier dataset. Figures 9-12 show the fitted PDF's, CDF's, and PP plots for the BMOWR model and the other distributions. Tables 13 and 14 provide the ML estimates, TSE estimates, and SEs of the unknown parameters for the example data. Additionally, the ML predictors and bounds for future observations under two-sample prediction are given in Table 15.

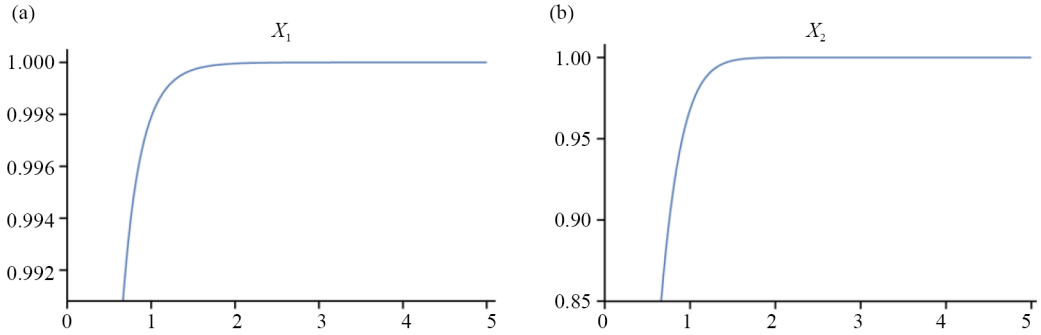

Figure 9. The probabilities from the classifier dataset, showing the marginal distributions

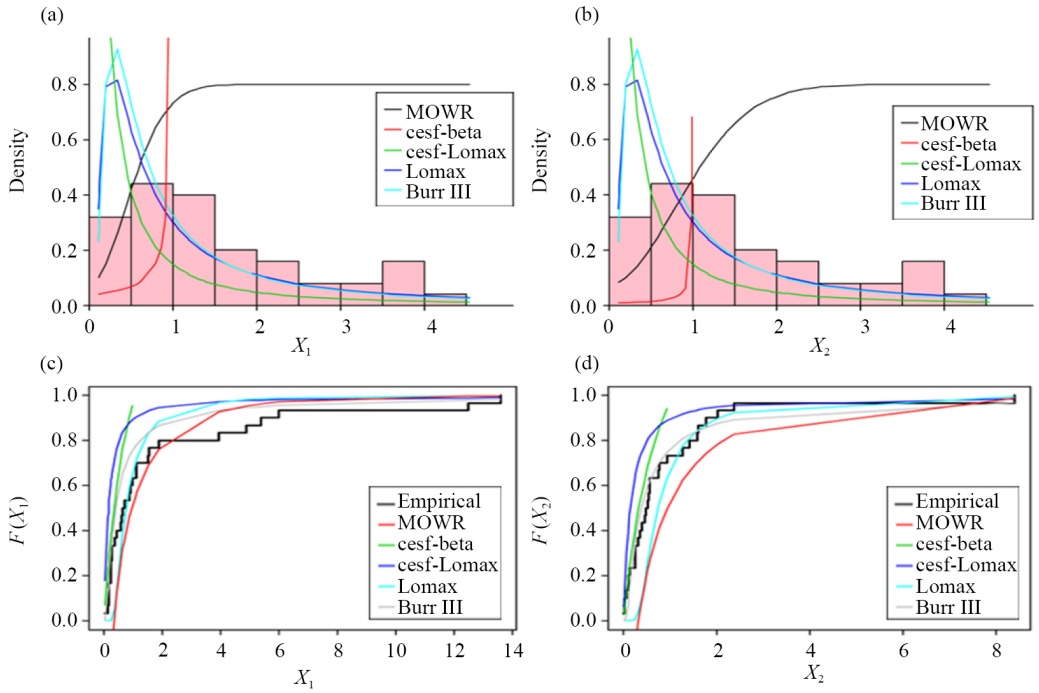

Figure 10. Estimated PDF and estimated distributions of the models for the dataset

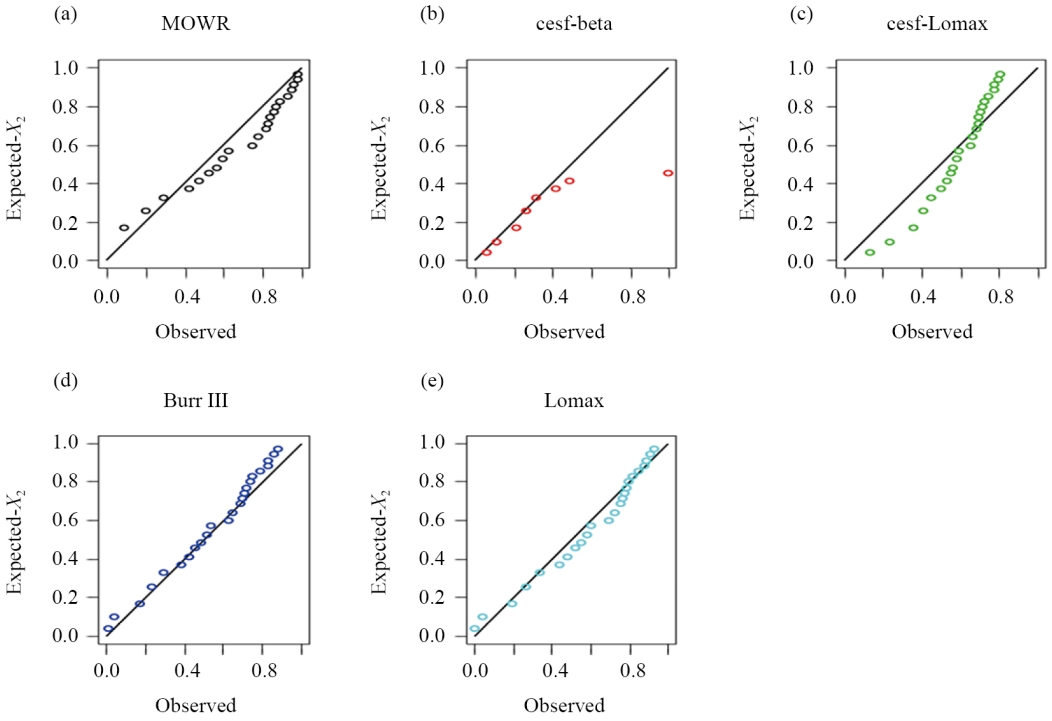

Figure 11. The PP plots of the different models for the dataset X_1

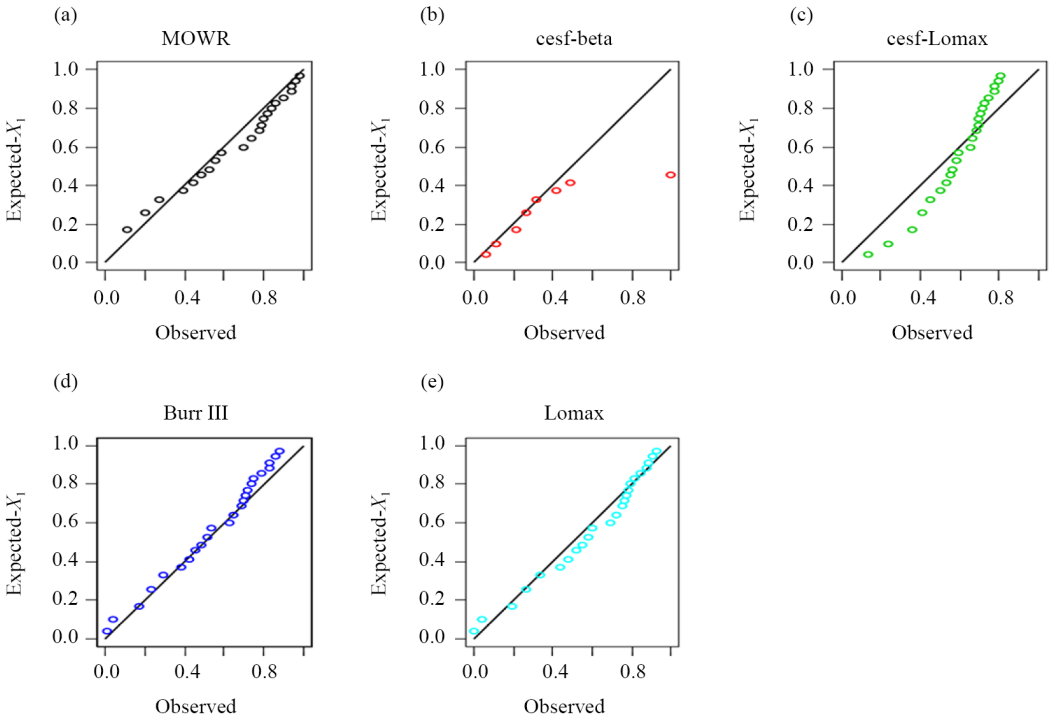

Figure 12. The PP plots of the different models for the dataset X_2

Table 13. MLE estimates, standard errors of the parameters (Case I and Case II)

n	Parameters	Estimate		SE	
		Case I	Case II	Case I	Case II
30	θ	0.1516	−4.686e-6	0.4586	0.0099
	α_1	0.8534	0.68815	0.4600	0.1111
	α_2	1.4736	0.7784	0.4698	0.1206
	β_1	0.5952	0.8127	0.1914	0.0127
	β_2	0.5878	0.9397	0.0875	0.0396
	μ_1	0.0659	0.4891	0.4989	0.0887
	μ_2	0.3759	0.3597	0.0240	0.0596
	λ_1	1.1904	0.8127	0.359	0.1270
	λ_2	1.0581	0.9397	0.1561	0.0396

Table 14. TSE estimates, standard errors of the parameters (Case I and Case II)

n	Parameters	Estimate		SE	
		Case I	Case II	Case I	Case II
30	θ	−0.0041	−0.0104	0.0058	0.0003
	α_1	0.3805	0.7993	0.3807	0.0005
	α_2	0.5150	0.8996	0.3552	0.0004
	β_1	1.4120	0.8998	0.4398	0.0005
	β_2	0.4036	0.8012	0.3639	0.0006
	μ_1	0.4895	0.4006	0.0891	0.0006
	μ_2	0.5556	0.8005	0.2369	0.0007
	λ_1	1.4120	0.9000	0.4398	0.0004
	λ_2	0.8249	0.7999	0.0249	0.0005

Table 15. ML predictive and bounds of future observations under two-sample prediction

n	s	$\widehat{y}_{(s)}$	Predictor	UL	LL	Length
30	5	$\widehat{y}_{1(s)}$	1.4819	5.0621	0.3217	4.7403
		$\widehat{y}_{2(s)}$	0.8571	1.7877	0.3104	1.4773
	8	$\widehat{y}_{1(s)}$	3.3637	6.6465	1.1376	5.5088
		$\widehat{y}_{2(s)}$	1.8931	2.1367	0.7217	1.4150
	10	$\widehat{y}_{1(s)}$	5.5417	7.7022	1.8960	5.8061
		$\widehat{y}_{2(s)}$	2.9168	2.3770	0.9630	1.4139

8. Concluding remarks

This paper successfully introduced and extensively investigated a novel univariate and bivariate distribution: the BMOWR distribution, which is constructed using the FGM copula. Our theoretical exploration revealed that the BMOWR offers significant flexibility in modeling various bivariate hazard rate shapes, including increasing, decreasing, and bathtub curves. Furthermore, this model proved capable of effectively capturing diverse dependence structures essential for bivariate lifetime data analysis.

Regarding parameter estimation, a comprehensive comparison between MLE and TSE methods demonstrated their efficacy in providing robust and efficient estimation strategies for the BMOWR distribution's unknown parameters. Furthermore, two MLE-based predictors were successfully derived for future observations. The theoretical results and

proposed procedures were rigorously validated through a numerical illustration via Markov Chain Monte Carlo (MCMC) simulation study, confirming their consistency and performance.

The superior performance and practical applicability of the proposed BMOWR distribution were demonstrated through the analysis of two real-world datasets. This empirical evidence, along with the detailed comparative study against other established bivariate models, establishes the BMOWR distribution as a highly valuable and robust alternative for accurately modeling and understanding complex bivariate lifetime data in fields such as reliability engineering.

9. Future research

Future research should focus on enhancing the model's robustness and applicability. This includes exploring methods for handling missing data, developing automated model selection and validation procedures, and incorporating Bayesian approaches to address parameter uncertainty. Investigating computational efficiency, extending the model to higher dimensions or different data types, and performing a detailed moment analysis are also crucial. For lifetime data analysis, extending the model to handle competing risks and time-varying covariates should be considered. Furthermore, exploring the model's performance under various copula functions, censoring schemes, and parameterizations would provide a more comprehensive understanding. We believe that exploring the construction of BMOWR distributions with more flexible copulas represents a natural and important direction for future research. Assessing the robustness of the estimators and the model's performance under copula misspecification is a crucial aspect for practical applications. This represents valuable area for future research. Finally, exploring real-world applications and conducting case studies will demonstrate the model's practical utility and solidify its contributions to the field.

Acknowledgments

The author would like to thank the Editor-in-Chief and the referee for their constructive comments, which significantly improved the paper.

Data availability

The data used to support the findings of this study are included within the article.

Conflict of interest

The authors declare no conflicts of interest.

References

[1] Marshall AW, Olkin I. A new method for adding a parameter to a family of distributions with application to the exponential and Weibull families. *Biometrics*. 1997; 84(3): 641-652.

[2] Meintanis SG. Test of fit for Marshall-Olkin distributions with applications. *Journal of Statistical Planning and Inference*. 2007; 137(12): 3954-3963.

[3] Cordeiro GM, De Castro M. A new family of generalized distributions. *Journal of Statistical Computation and Simulation*. 2011; 81(7): 883-898.

[4] Alzaghal A, Famoye F, Lee C. Exponentiated T-X family of distributions with some applications. *International Journal of Statistics and Probability*. 2013; 2(3): 31-49.

[5] Alzaatreh A, Famoye F, Lee C. Weibull-Pareto distribution and its applications. *Communications in Statistics Theory and Methods*. 2013; 42(9): 1673-1691.
[6] Alzaatreh A, Lee C, Famoye F. A new method for generating families of continuous distributions. *Metron*. 2013; 71(1): 63-79.
[7] Alshangiti AM, Kayid M, Alarfaj B. A new family of Marshall-Olkin extended distributions. *Journal of Computational and Applied Mathematics*. 2014; 271: 369-379.
[8] Okasha HM, Kayid M. A new family of Marshall-Olkin extended generalized linear exponential distribution. *Journal of Computational and Applied Mathematics*. 2016; 296: 576-592.
[9] Aljarrah M, Lee C, Famoye F. On generating *T-X* family of distributions using quantile functions. *Journal of Statistical Distributions and Applications*. 2014; 1(1): 2.
[10] Bourguignon M, Silva RB, Cordeiro GM. The Weibull-G family of probability distributions. *Journal of Data Science*. 2014; 12(1): 53-68.
[11] Salem HM, Selim MA. The generalized Weibull-exponentiated distribution: Properties and applications. *International Journal of Statistics and Applications*. 2014; 4(2): 102-112.
[12] Tahir MH, Zubair M, Mansoor M, Cordeiro GM, Alzaatreh A. A new Weibull-G family of distributions. *Hacettepe Journal of Mathematics and Statistics*. 2016; 45(2): 629-647.
[13] Jamal F, Nasir MA. Some new members of the *T-X* family of distributions. In: *Proceedings of the 17th International Conference on Statistical Sciences*. Lahore, Pakistan: Islamic Countries Society of Statistical Sciences (ISOSS); 2019. p.113-120.
[14] Nadarajah S, Rocha R. Newdistns: An R package for new families of distributions. *Journal of Statistical Software*. 2016; 69(10): 1-32.
[15] Nadarajah S, Rocha R. Newdistns: Computes Pdf, Cdf, quantile and random numbers, measures of inference for 19 general families of distributions. *Journal of Statistical Software*. 2016; 69(10): 1-32.
[16] Pakungwati RM, Widyaningsih Y, Lestari D. Marshall-Olkin extended inverse Weibull distribution and its application. *Journal of Physics: Conference Series*. 2018; 1108(1): 012114.
[17] Ishaq AI, Abiodun AA. The Maxwell-Weibull distribution in modeling lifetime datasets. *Annals of Data Science*. 2020; 7(4): 639-662.
[18] Almetwally EM, Sabry MA, Alharbi R, Alnagar D, Mubarak SA, Hafez EH. Marshall-Olkin alpha power Weibull distribution: Different methods of estimation based on type-I and type-II censoring. *Complexity*. 2021; 2021(1): 5533799.
[19] Almetwally EM, Afify AZ, Hamedani G. Marshall-Olkin alpha power Rayleigh distribution: Properties, characterizations, estimation and engineering applications. *Pakistan Journal of Statistics and Operation Research*. 2021; 17(3): 745-760.
[20] Elgarhy M, Johannssen A, Kayid M. An extended Rayleigh Weibull model with actuarial measures and applications. *Heliyon*. 2024; 10(11): e32143.
[21] Singh SK, Singh U, Sharma VK. Bayesian estimation and prediction for flexible Weibull model under type-II censoring scheme. *Journal of Probability and Statistics*. 2013; 2013(1): 146140.
[22] Singh SK, Singh U, Sharma VK. Bayesian prediction of future observations from inverse Weibull distribution based on type-II hybrid censored sample. *International Journal of Advanced Statistics and Probability*. 2013; 1(2): 32-43.
[23] Sklar M. *N-Dimensional Distribution Functions and Their Margins.* Paris: Université Paris 8; 1959.
[24] Genest C, Remillard B, Beaudoin D. Goodness-of-fit tests for copulas: A review and a power study. *Insurance: Mathematics and Economics*. 2009; 44(2): 199-213.
[25] Kojadinovic I, Yan J, Holmes M. Fast large-sample goodness-of-fit tests for copulas. *Statistica Sinica*. 2011; 21(2): 841-871.
[26] Ateya SF, Al-Alazwari AA. A new multivariate generalized exponential distribution with application. *Far East Journal of Theoretical Statistics*. 2013; 45(1): 51-70.
[27] Abd Elaal MK, Kalantan ZI. Study the modeling of bivariate Weibull Rayleigh distribution with Gaussian copula. *Applied Mathematical Sciences*. 2018; 12(25): 1209-1217.
[28] Kalantan Z, Abd Elaal MK. Bivariate Weibull exponential model based on Gaussian copula. In: *Proceedings of the Third International Conference on Computing, Mathematics and Statistics (iCMS2017)*. Singapore: Springer; 2019. p.277-285.

[29] Kalantan ZI, Abd Elaal MK. Parameters estimations on Bivariate Weibull G distributions: A new family. *Advances and Applications in Statistics*. 2019; 58(2): 77-122.
[30] Kalantan ZI, Abd Elaal MKA. Bivariate Weibull exponential model based on Gaussian copula. In: *Proceedings of the Third International Conference on Computing, Mathematics and Statistics (iCMS2017)*. Singapore: Springer; 2019. p.277-285.
[31] Oliveira RP, Achcar JA, Mazucheli J, Bertoli W. A new class of bivariate Lindley distributions based on stress and shock models and some of their reliability properties. *Reliability Engineering & System Safety*. 2021; 211: 107528.
[32] Mahmoud AAM, Refaey RM, Al-Dayian GR, El-Helbawy AA. Bivariate burr type III distribution: Estimation and prediction. *Journal of Advances in Mathematics and Computer Science*. 2021; 36(1): 16-36.
[33] Refaey RM, Al-Dayian GR, El-Helbawy AA, Mahmoud AAM. Bivariate compound exponentiated survival function of the Lomax distribution: Estimation and prediction. *Asian Journal of Probability and Statistics*. 2021; 15(4): 163-184.
[34] El-Sherpieny ESA, Almetwally EM, Muhammed HZ. Bivariate Weibull-G family based on copula function: Properties, bayesian and non-bayesian estimation and applications. *Statistics, Optimization Information Computing*. 2022; 10(3): 678-709.
[35] El-Sherpieny ES, Alrajhi HA, Hamdy MI, Hassan S. Bivariate Weibull-G family based on copula function: Properties, bayesian and non-Bayesian estimation and applications. *Mathematical Problems in Engineering*. 2022; 2022: 1-15.
[36] Pathak AK, Arshad M, Azhad QJ, Khetan M, Pandey A. A novel bivariate generalized Weibull distribution with properties and applications. *American Journal of Mathematical and Management Sciences*. 2023; 42(4): 279-306.
[37] Binhimd S, Kalantan ZI, El-Helbawy AA, Al-Dayian GR, Mahmoud AAAM, Refaey RM, et al. A new bivariate survival model: The Marshall-Olkin bivariate exponentiated Lomax distribution with modeling bivariate football scoring data. *Axioms*. 2024; 13(11): 1-20.
[38] Nelsen RB. *An Introduction to Copulas*. 2nd ed. New York: Springer; 2006.
[39] Fayomi A, Refaey RM, Al-Dayian GR, El-Helbawy A, Mahmoud AAM, Abd Elaal M. Bivariate Lomax distribution based on Clayton copula: Estimation and prediction. *Journal of Statistics Applications and Probability*. 2024; 13(4): 1321-1337.
[40] Mahmoud AAM, Khashab RH, Kalantan ZI, Binhimd SMS, Alghamdi AS, Nassr SG. On bivariate compound exponentiated survival function of the beta distribution: Estimation and prediction. *Journal of Radiation Research and Applied Sciences*. 2024; 17(2): 100886.
[41] Kojadinović I, Yan J. Comparison of three semiparametric methods for estimating dependence parameters in copula models. *Insurance: Mathematics and Economics*. 2010; 47(1): 52-64.
[42] Genest C, Rémillard B. Validity of the parametric bootstrap for goodness-of-fit testing in semiparametric models. *Annals of the Henri Poincaré Institute: Probability and Statistics*. 2008; 44(6): 1096-1127.